

Supporting Information

The effect of weighted averages when determining speciation and structure-property relationships of europium(III) dipicolinate complexes

Patrick R. Nawrocki, Nicolaj Kofod, Mikkel Juelsholt, Kirsten M. Ø. Jensen and
Thomas Just Sørensen*

Department of Chemistry & Nano-Science Center, University of Copenhagen, Universitetsparken 5,
2100 København Ø, Denmark

Table of Contents

| | |
|---|------------|
| SAMPLE PREPARATION | S4 |
| LUMINESCENT LIFETIME | S5 |
| ABSORPTION SPECTROSCOPY | S7 |
| Fitting ${}^5D_0 \leftarrow {}^7F_0$ | S13 |
| Excitation Spectroscopy | S15 |
| Raw spectra..... | S15 |
| Comparing absorption and excitation spectra | S18 |
| Emission Spectroscopy | S19 |
| Raw spectra..... | S19 |
| Spectra normalized by excitation band and τ_{H_2O} | S21 |
| Spectroscopy Isotherms | S27 |
| NMR Spectroscopy | S30 |
| Total Scattering – Pair Distribution Functions | S32 |
| I(Q) | S32 |
| DYNAFIT SPECIATION MODELLING | S36 |
| Absorption spectroscopy | S36 |
| Optimized Parameters..... | S37 |
| 100 × Correlation Matrix | S37 |
| Confidence Interval Profiles | S37 |
| Absorption speciation | S38 |
| Comparison of speciation model with emission isotherms | S40 |
| Excitation..... | S41 |
| NMR..... | S42 |
| Lifetimes & q..... | S42 |

| | |
|---|------------|
| X-RAY SCATTERING DATA AND MODELS FROM SPECIATION | S43 |
| EuDPA structures and modelled PDF's at varying q | S43 |
| Total scattering PDF models and data quality | S43 |
| Model and data of EuDPA samples..... | S45 |
| Models and fit with $q = 33.5$ | S46 |
| Transition energies | S47 |
| Emission probabilities ${}^5D_0 \rightarrow {}^7F_J, J = 0-6$ | S48 |

Sample preparation

Mw(Eu₂O₃): 351.926 g/mol

Mw(2,6-pyridinedicarboxylic acid): 167.12 g/mol

Europium stock preparation – 5 ml. All experiments are conducted at ambient temperatures.

Table S1 – Calculated and measured compound amounts.

| C(mole/L) Eu ³⁺ | V(L) | n(mole) Eu ³⁺ | m(g) Eu ₂ O ₃ | w(mg) | Weighed (mg)±0. |
|-------------------------------|------|-----------------------------|--|-------|-----------------|
| 0.1 | 0.02 | 0.002 | 0.3519 | 351.9 | 352.1 |

| Eu:DPA (1:X) | C(DPA) | n(mol) eu | w(g) DPA | w(mg) | weighed (mg) ±0.1 |
|--------------|--------|-----------|----------|--------|-------------------|
| 0.00 | 0 | 0 | 0.0000 | 0 | 0 |
| 0.25 | 0.005 | 0.000025 | 0.0042 | 4.178 | 4.3 |
| 0.50 | 0.01 | 0.00005 | 0.0084 | 8.356 | 8.2 |
| 0.75 | 0.015 | 0.000075 | 0.0125 | 12.534 | 12.6 |
| 1.00 | 0.02 | 0.0001 | 0.0167 | 16.712 | 16.7 |
| 1.25 | 0.025 | 0.000125 | 0.0209 | 20.89 | 20.9 |
| 1.50 | 0.03 | 0.00015 | 0.0251 | 25.068 | 25.2 |
| 1.75 | 0.035 | 0.000175 | 0.0292 | 29.246 | 29.4 |
| 2.00 | 0.04 | 0.0002 | 0.0334 | 33.424 | 33.2 |
| 2.25 | 0.045 | 0.000225 | 0.0376 | 37.602 | 36.7 |
| 2.50 | 0.05 | 0.00025 | 0.0418 | 41.78 | 41.9 |
| 2.75 | 0.055 | 0.000275 | 0.0460 | 45.958 | 46.2 |
| 3.00 | 0.06 | 0.0003 | 0.0501 | 50.136 | 50.1 |
| 3.00 | 0.06 | 0.0003 | 0.0501 | 50.136 | 50.1 |

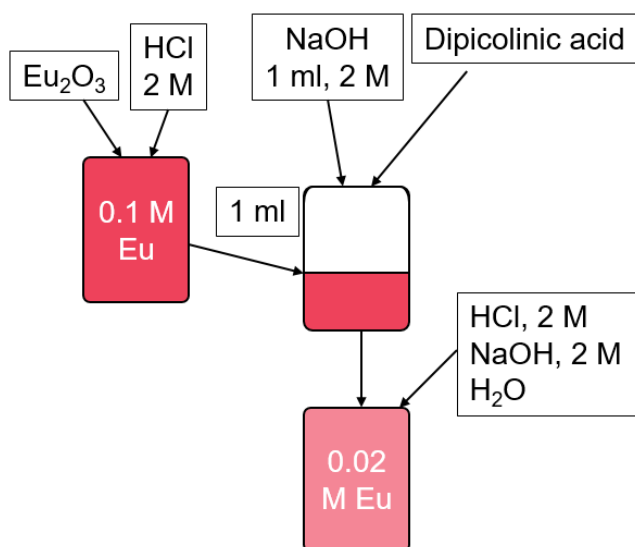


Figure S1 – Illustration of sample preparation procedure described.

Luminescent Lifetime

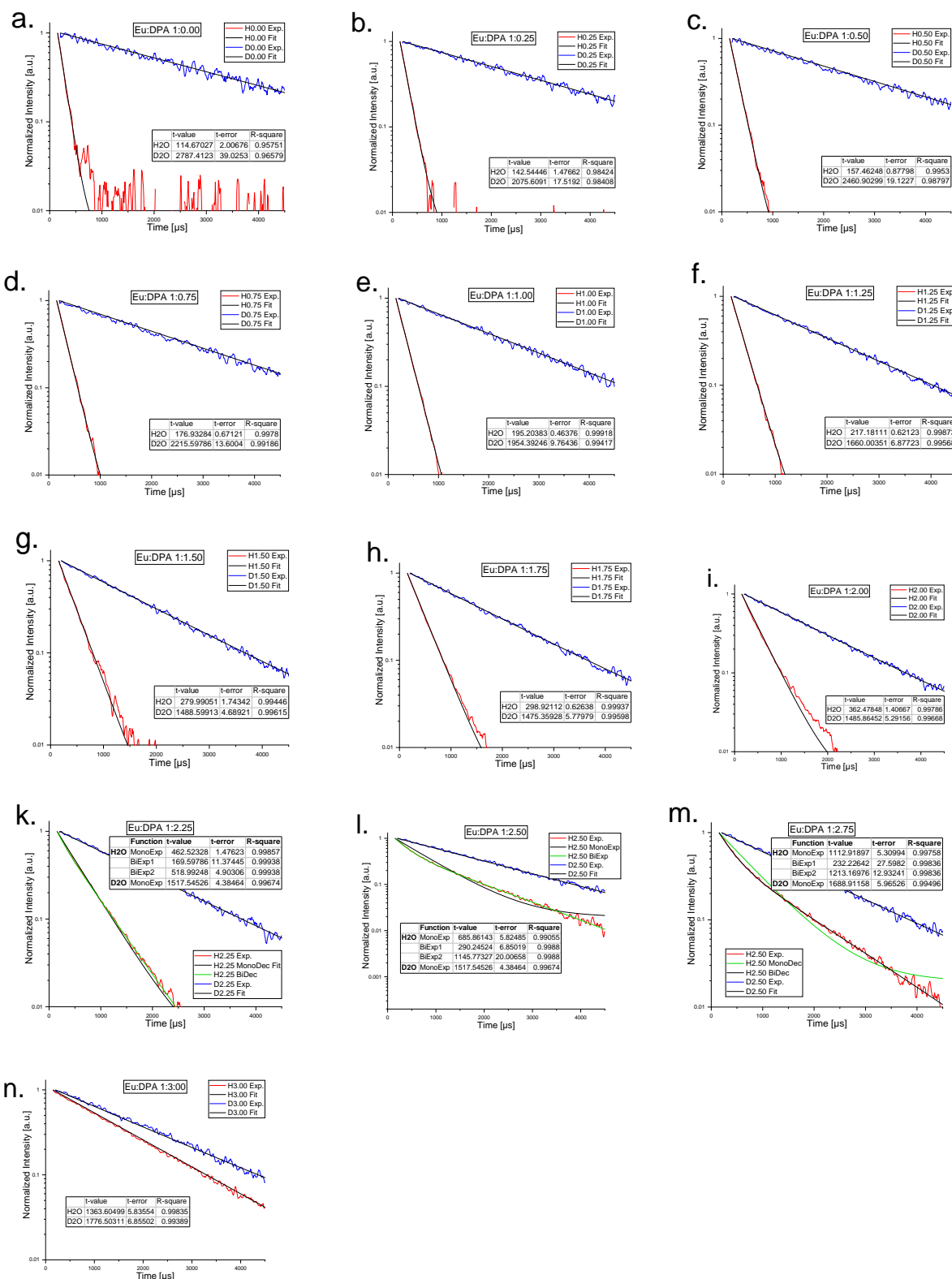


Figure S2 – a-n. Lifetime traces in H₂O and D₂O. $\lambda_{Ex} = 394$ nm, $\lambda_{Em} = 615$ nm.

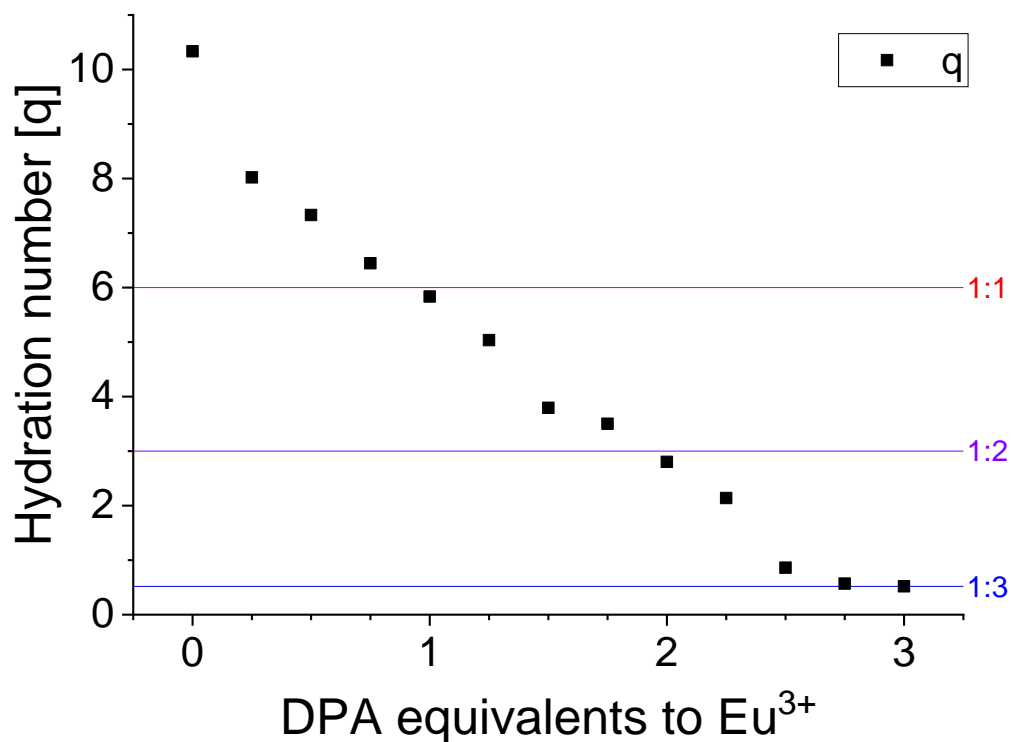
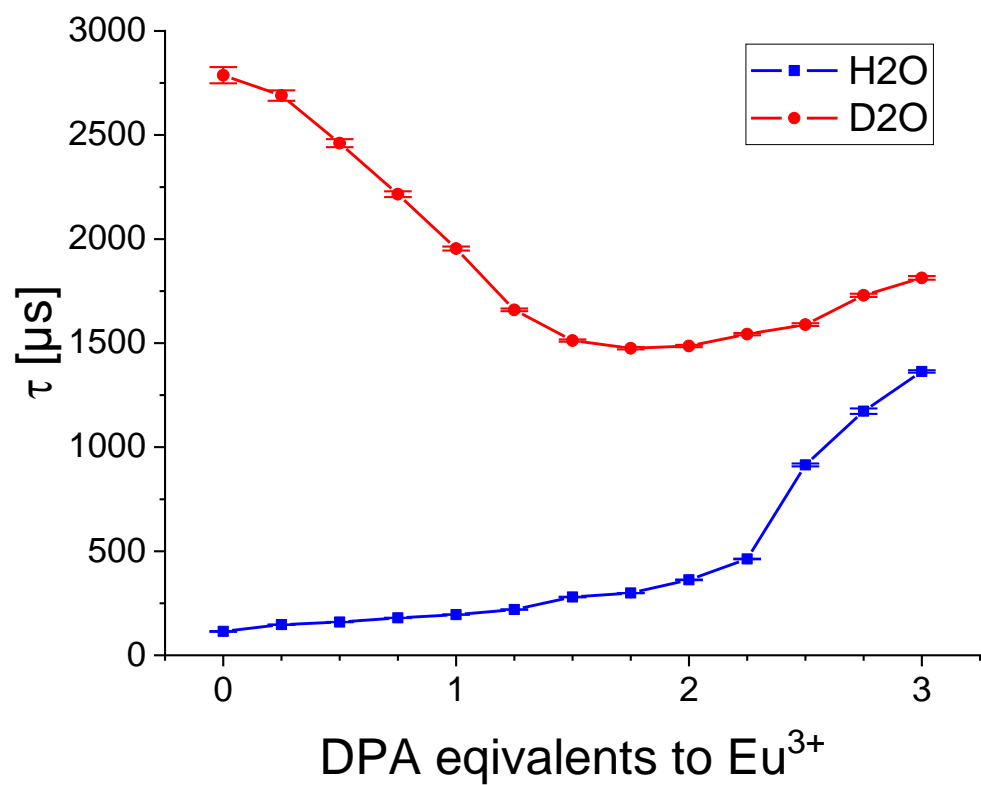


Figure S3 – Top: Fitted lifetimes of all samples. Bottom: Calculated q of all samples. The horizontal lines are indications of the expected q values of the three DPA complexes.

Absorption Spectroscopy

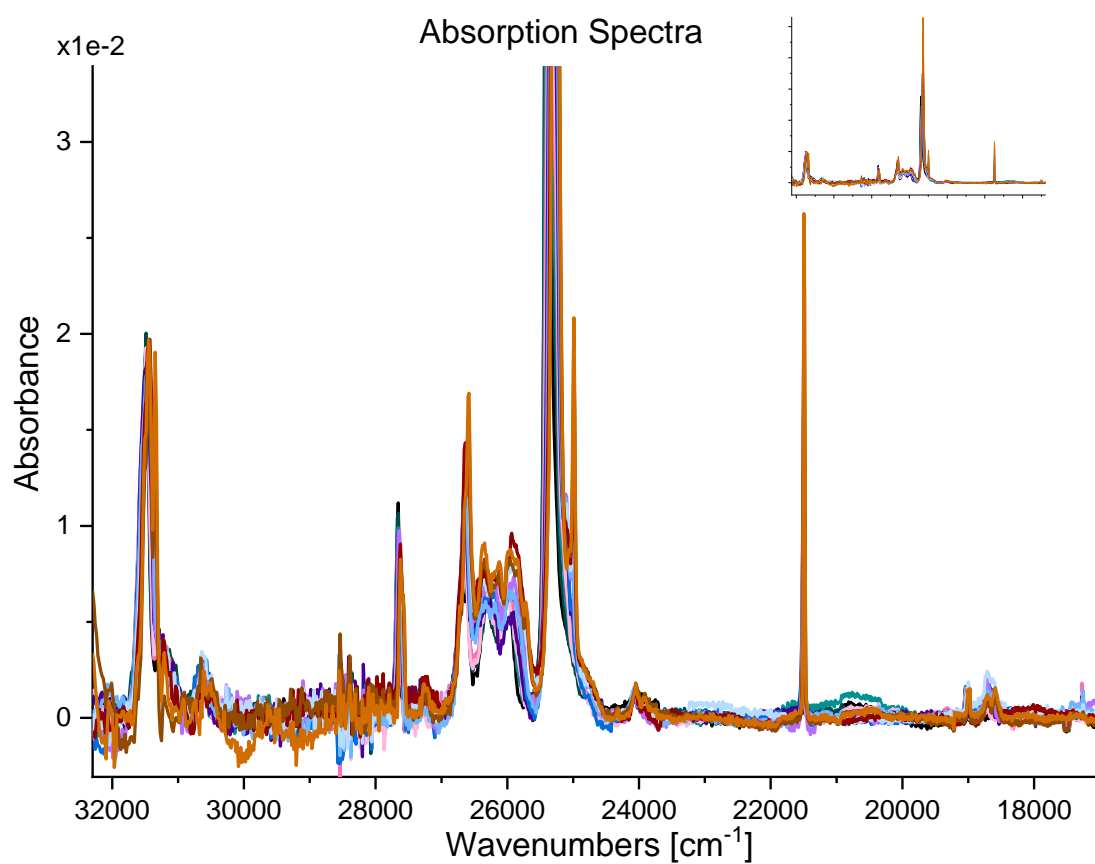


Figure S4 – Absorption spectrum of the europium(III) DPA titration series in H₂O at ambient temperature.

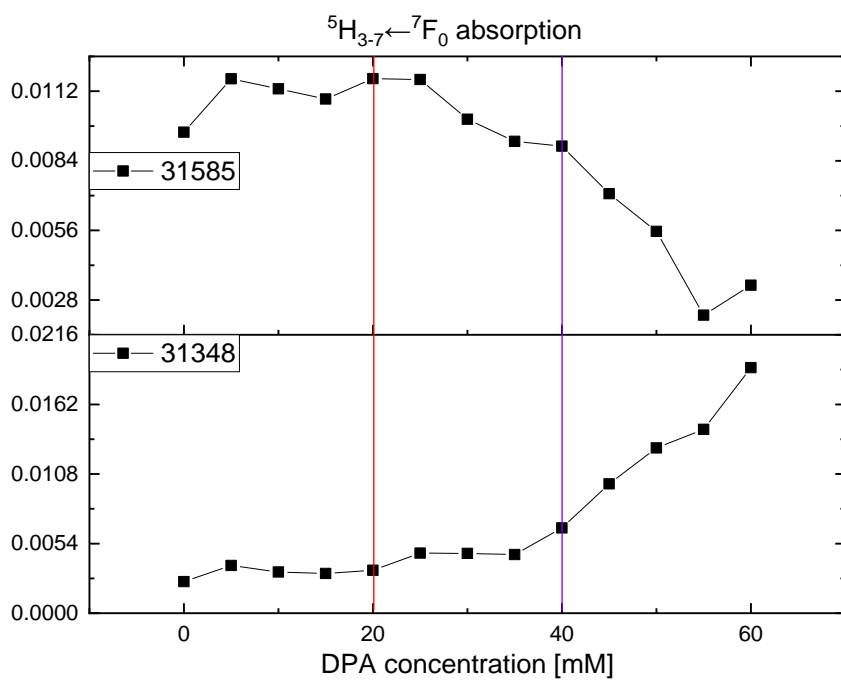
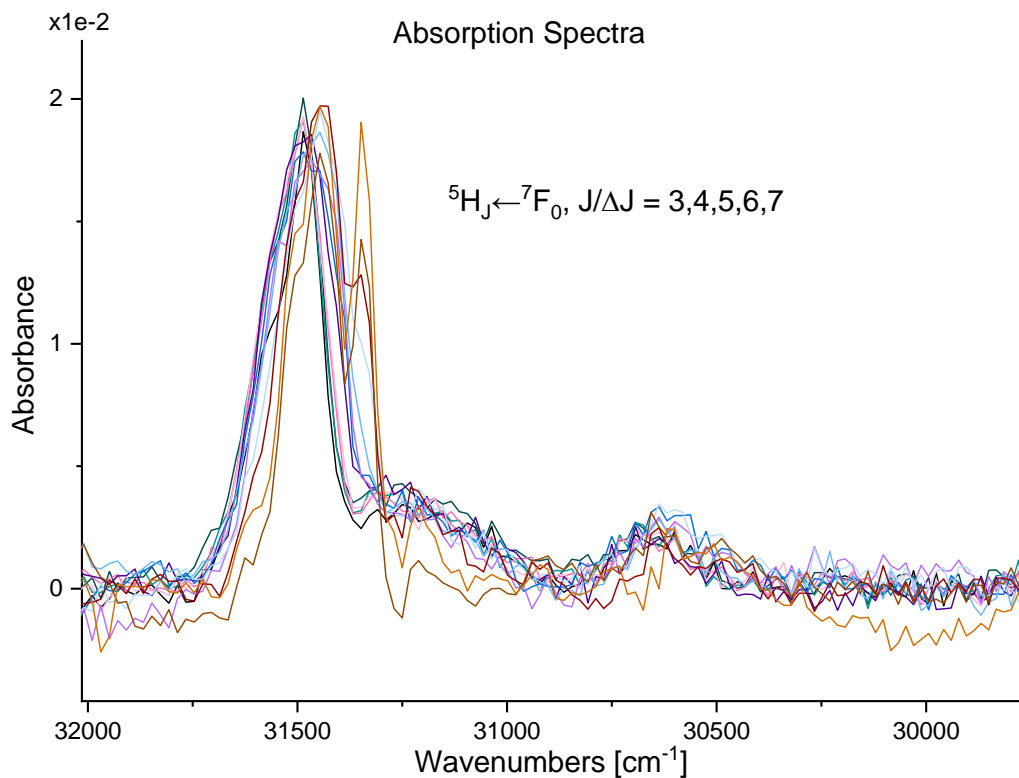


Figure S5 – Absorption spectrum of the ${}^5H_{3-7} \leftarrow {}^7F_0$ transition and the intensity isotherms at selected energies.

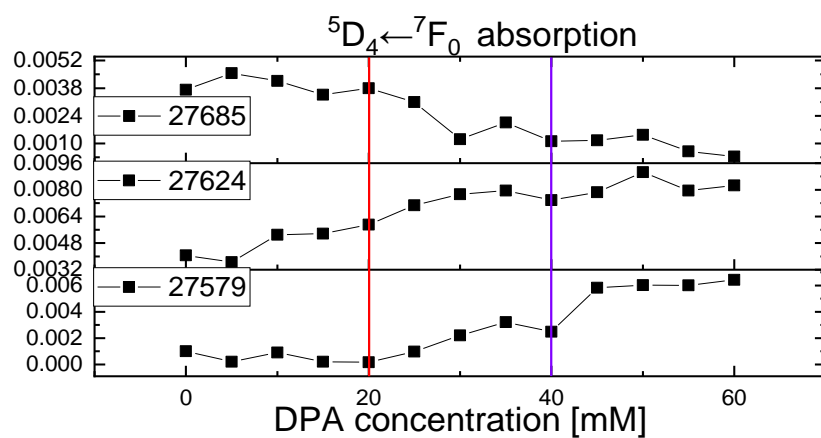
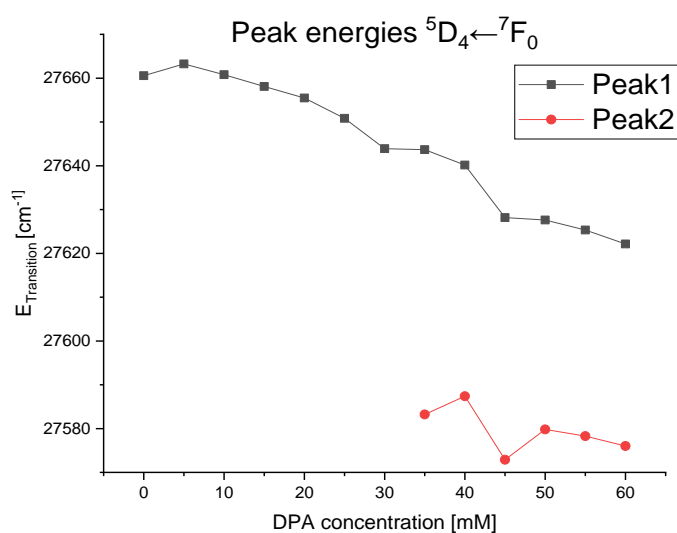
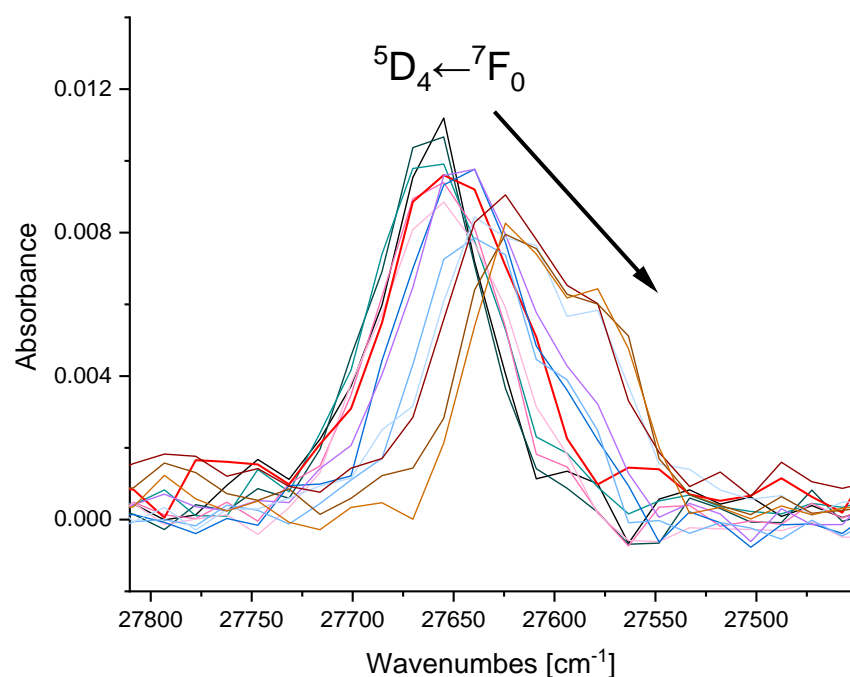


Figure S6 - Absorption spectrum of the ${}^5D_4 \leftarrow {}^7F_0$ transition, the energy of the peak center, the area of the peaks before and after being split, and the intensity isotherms at selected energies.

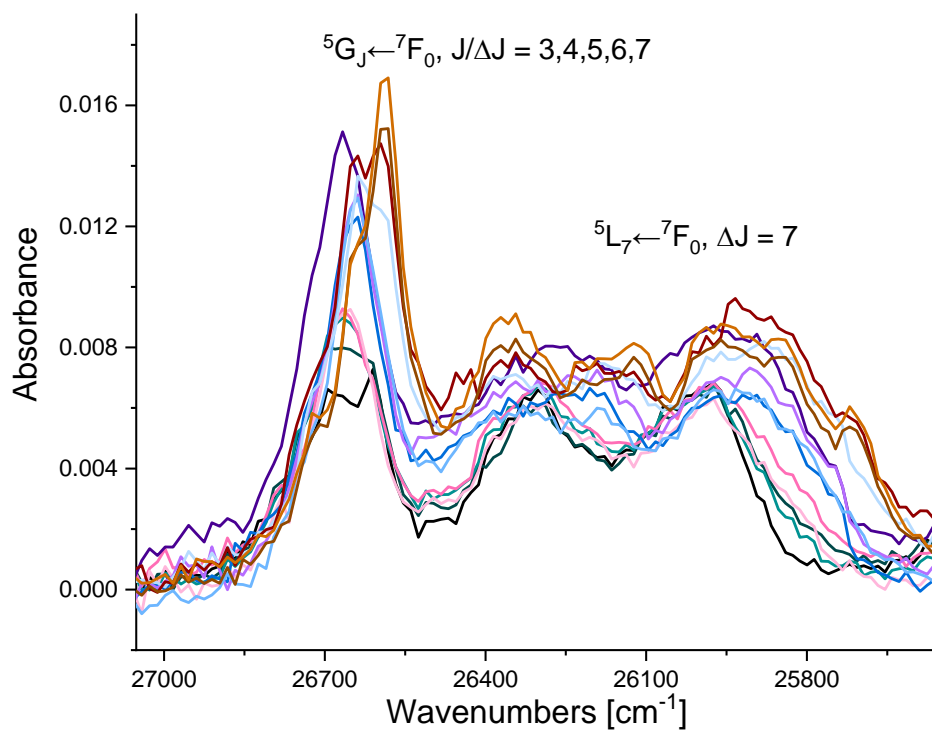


Figure S7 - Absorption spectrum of the ${}^5G_{3-7} \leftarrow {}^7F_0$ and ${}^5L_7 \leftarrow {}^7F_0$ transition.

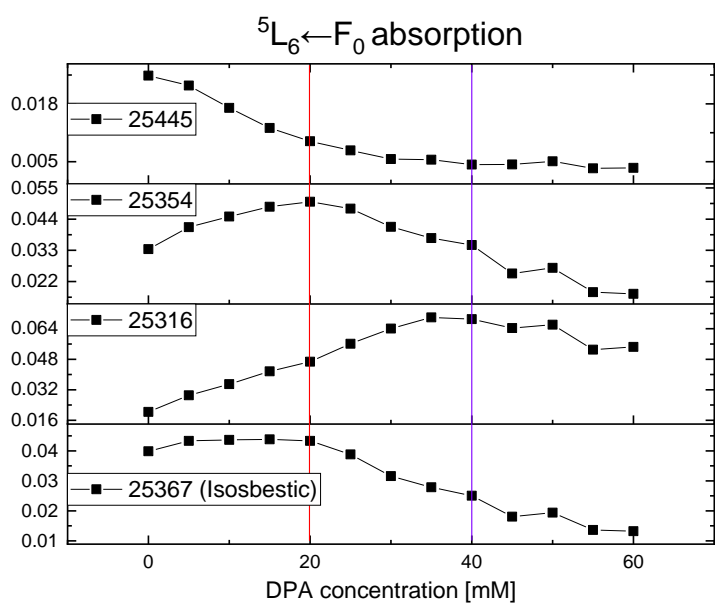
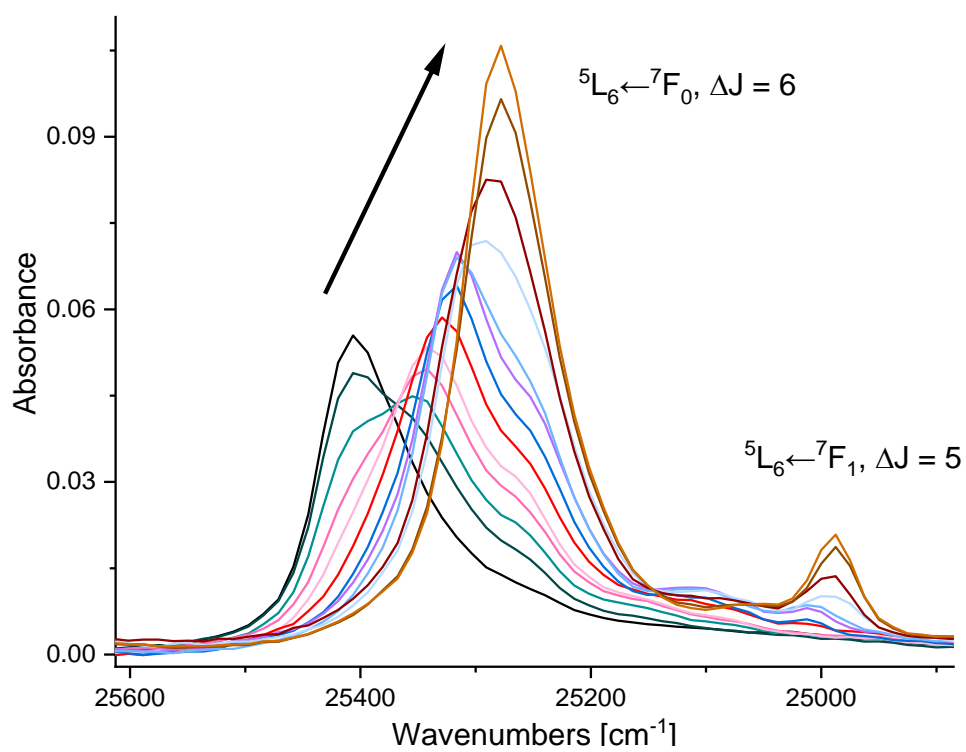


Figure S8 - Absorption spectrum of the ${}^5L_6 \leftarrow 7F_{0,1}$ transition and the intensity isotherms at selected energies.

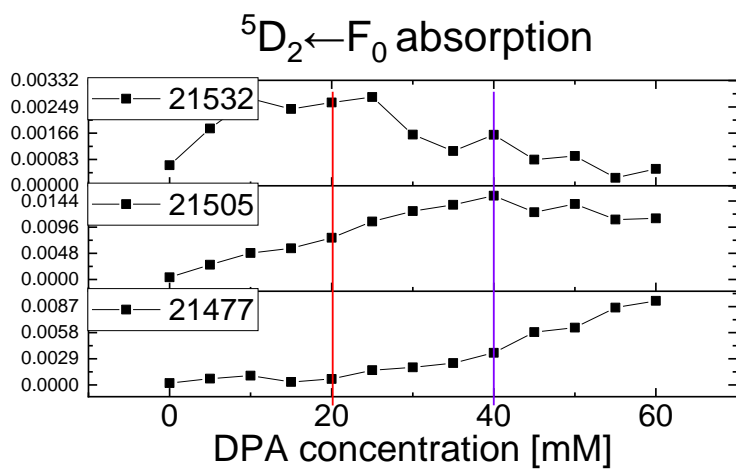
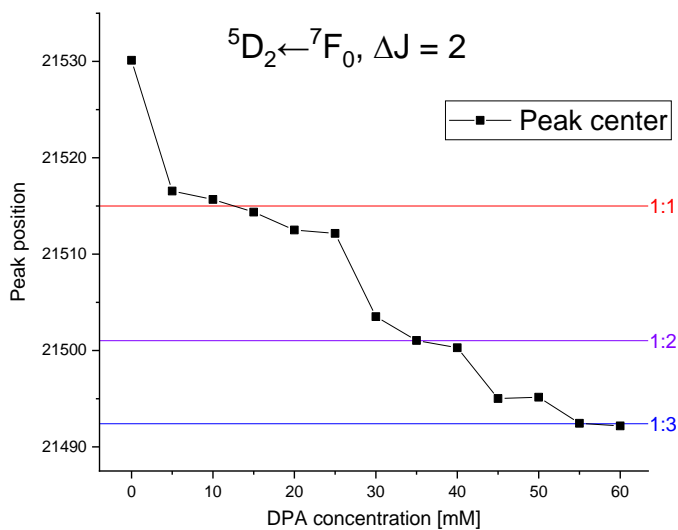
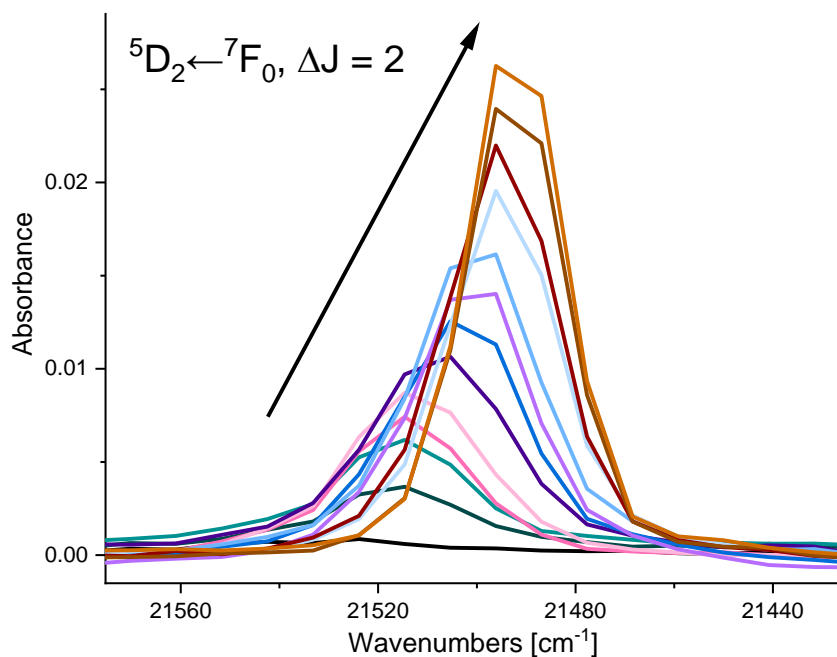


Figure S9 - Absorption spectrum of the ${}^5D_2 \leftarrow {}^7F_0$ transition, the energy of the peak center, the area of the peaks before and after being split, and the intensity isotherms at selected energies.

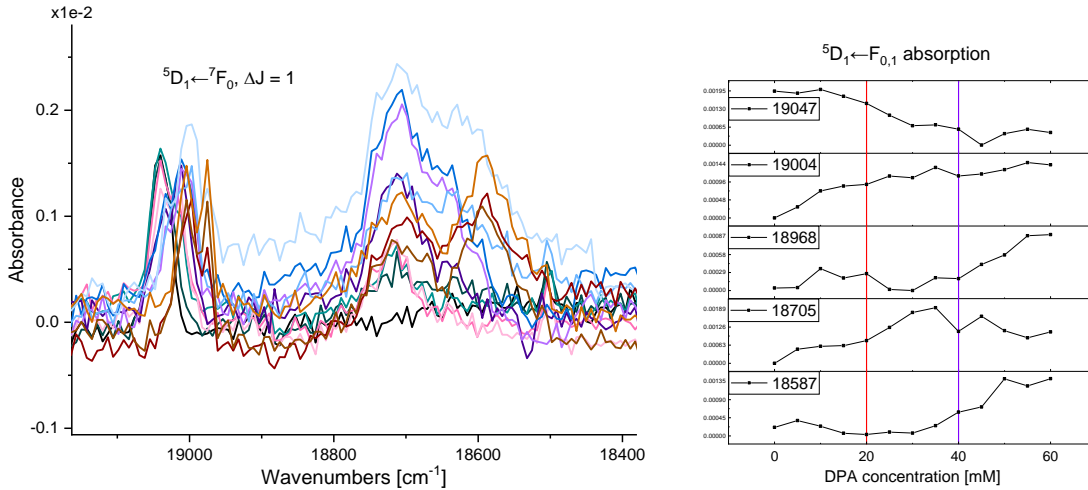


Figure S10 - Absorption spectrum of the ${}^5D_1 \leftarrow {}^7F_{0,1}$ transition, the energy of the peak center, the area of the peaks before and after being split, and the intensity isotherms at selected energies.

Fitting ${}^5D_0 \leftarrow {}^7F_0$

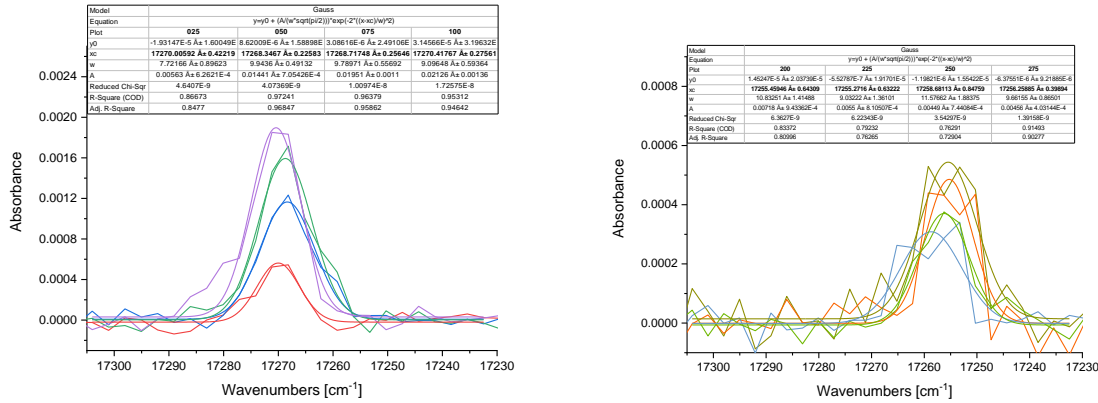


Figure S11 – Left: Gaussian fits of samples of 0.25, 0.50, 0.75 and 1.00 equivalents DPA to europium(III) for calculation of the absorbance peak of (1). Right: Gaussian fits of samples of 2.00, 2.25 and 2.75 equivalents DPA to europium(III) for calculation of the absorbance peak of (2).

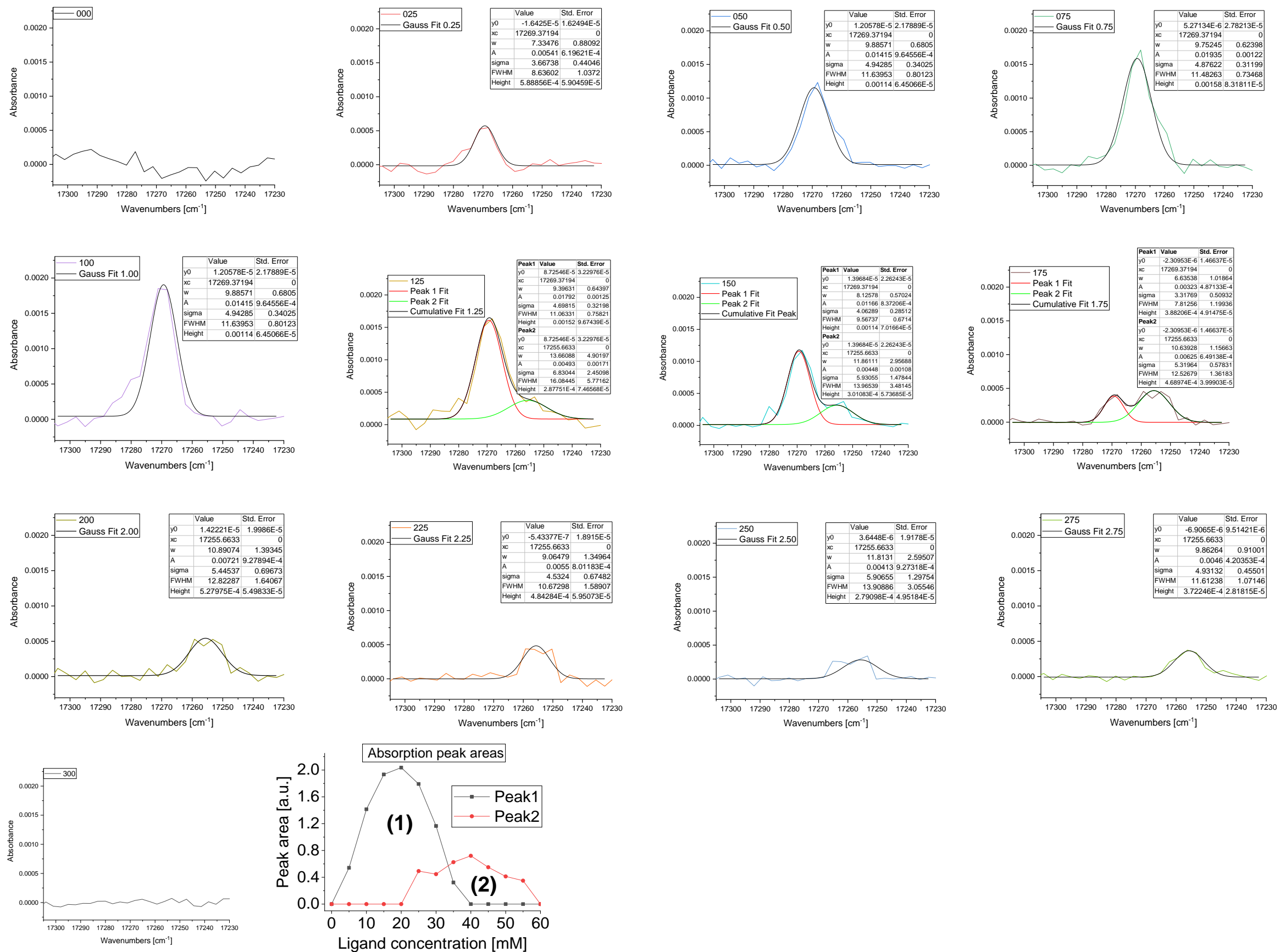


Figure S12 – Absorbance spectra of the ${}^5D_0 \leftarrow {}^7F_0$ band of individual samples, including Gaussian fits. The isotherms are shown in the bottom right figure.

Excitation Spectroscopy

Raw spectra

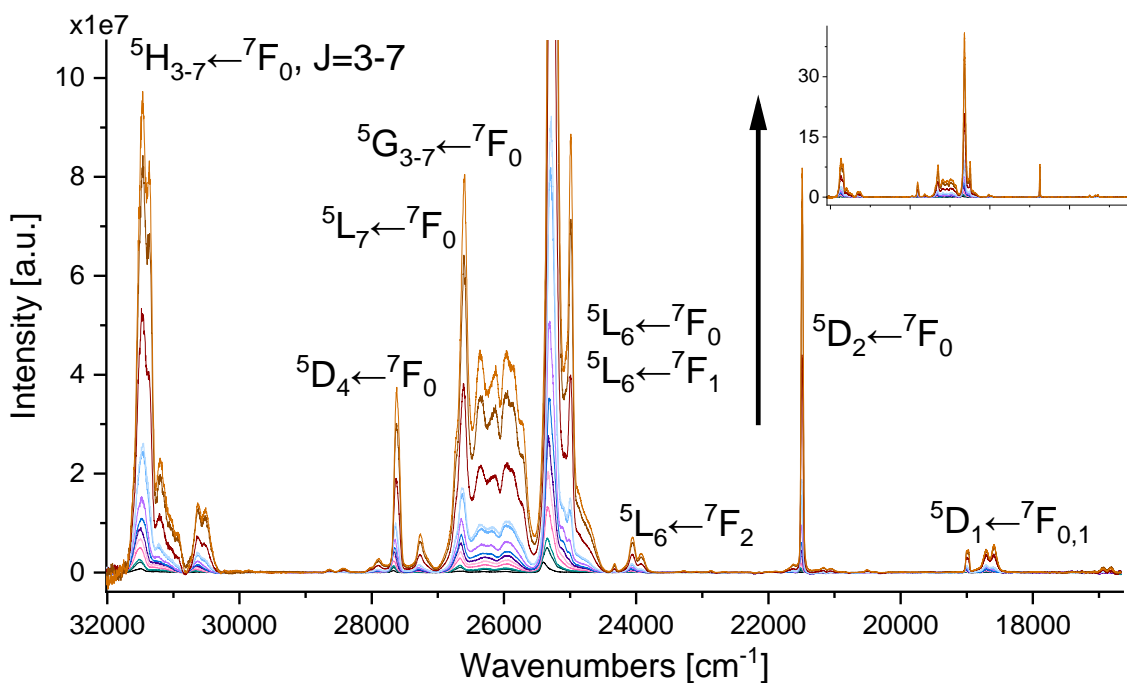
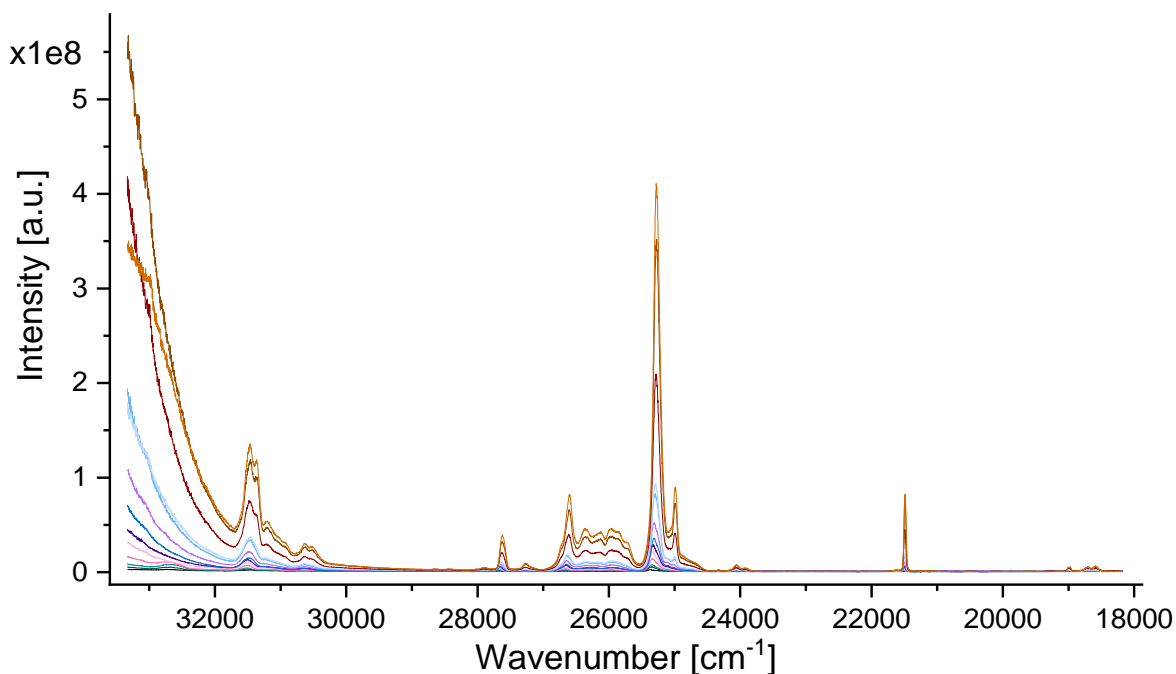


Figure S13 – Uncorrected (Top) and corrected (Bottom) excitation spectra of the europium(III) DPA titration series. The corrections include background subtraction and variations in the emission band intensity.

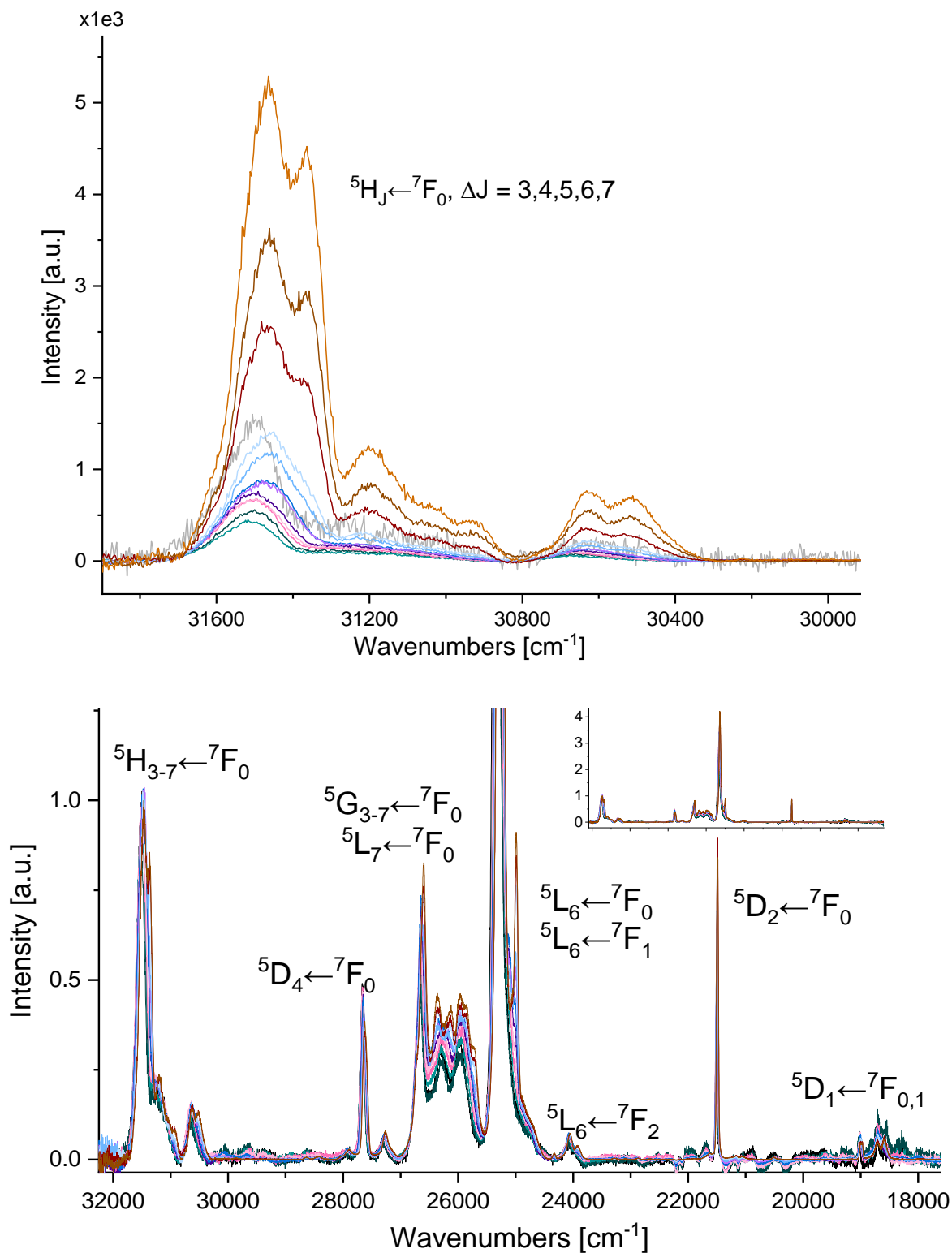


Figure S14 – Top: Excitation spectrum of the ${}^5\text{H}_{3-7} \leftarrow {}^7\text{F}_0$. Due to this bands invariance of absorption intensities across the titration series, the excitation spectra are corrected with respect to this bands area. Bottom: Excitation spectra after correction with ${}^5\text{H}_{3-7} \leftarrow {}^7\text{F}_0$ band area.

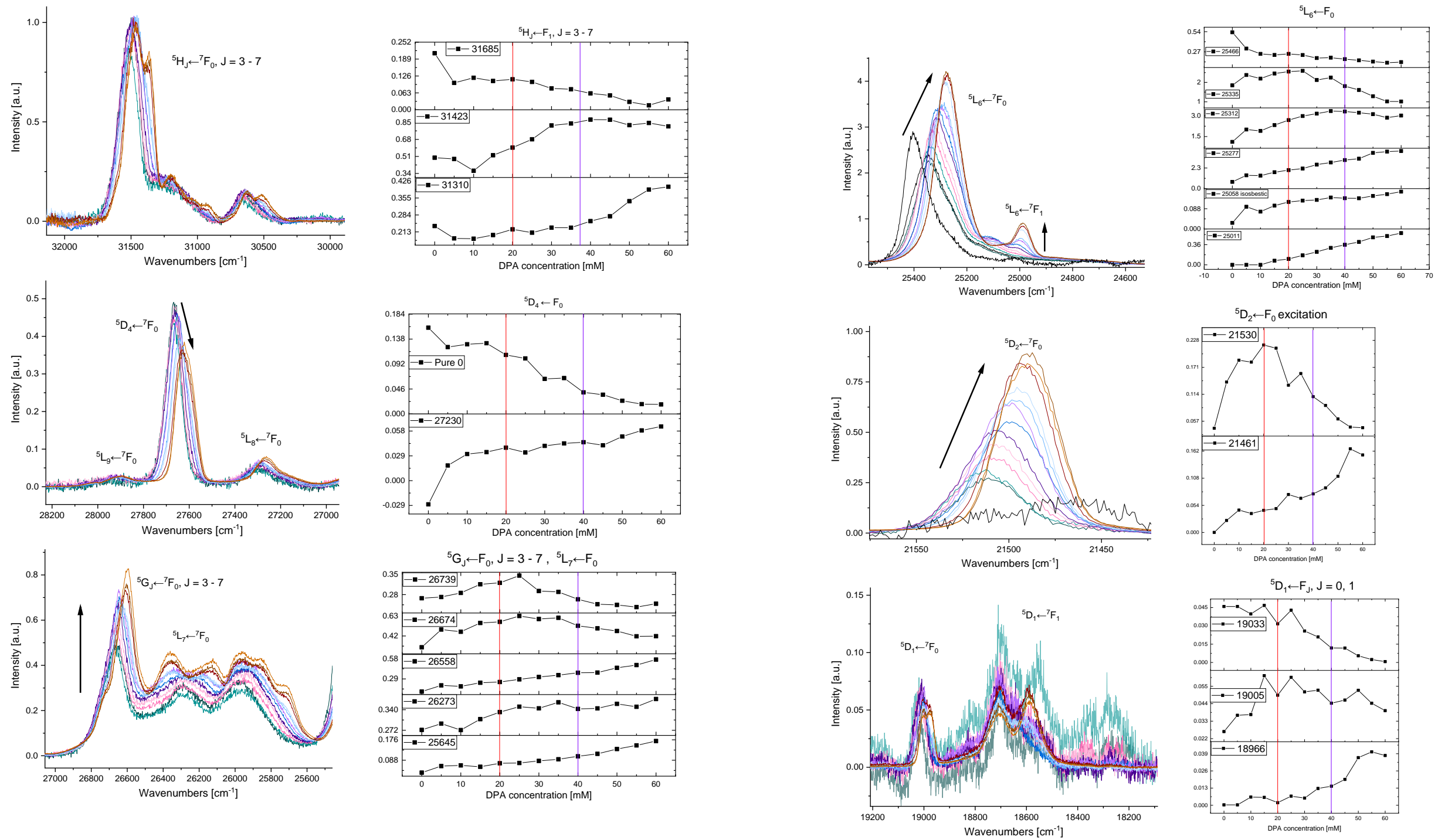


Figure S15 – Zoom-ins of the excitation spectra of the various spectral bands and the intensity isotherms at selected energies.

Comparing absorption and excitation spectra

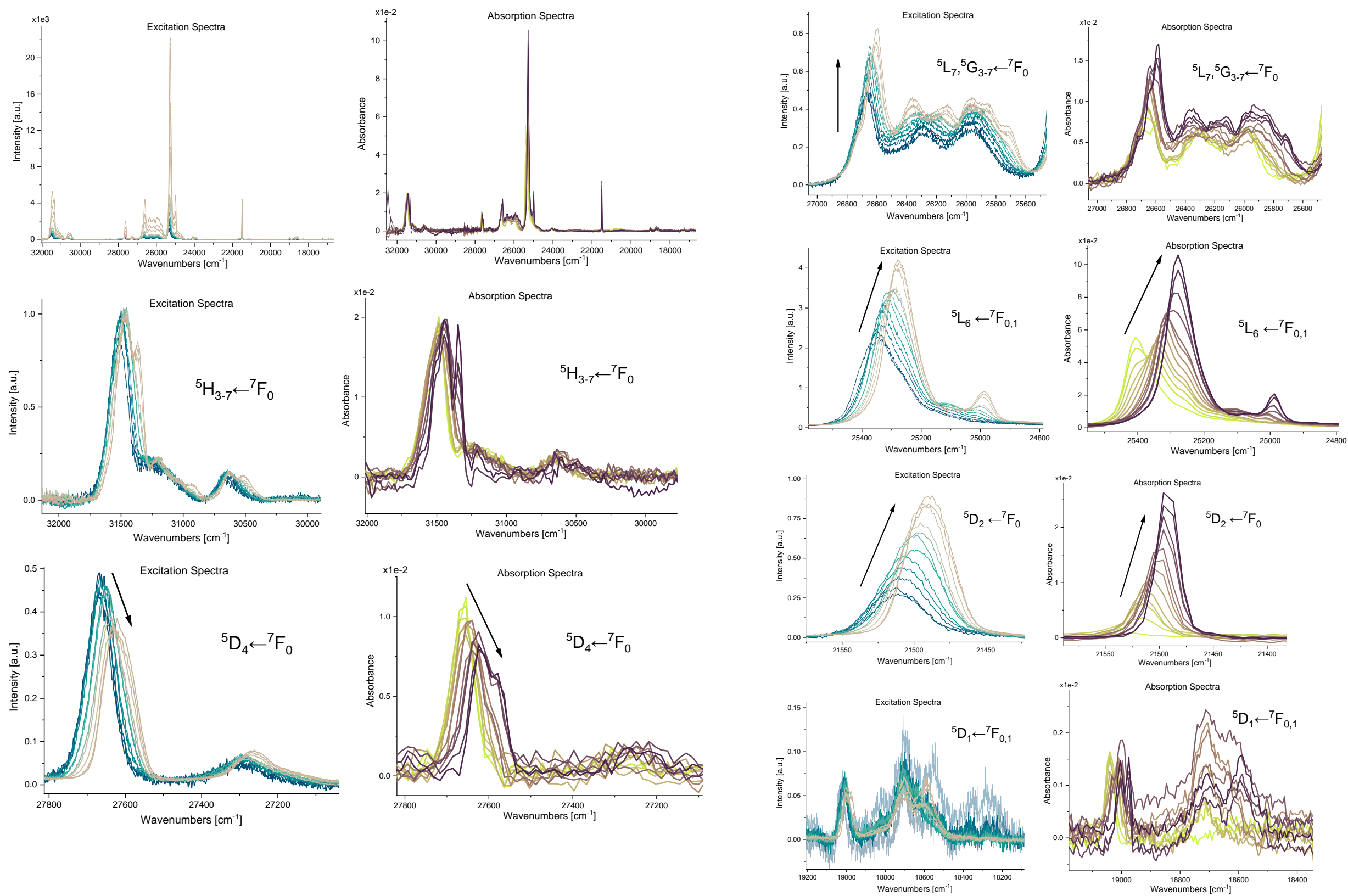


Figure S16 - Excitation and absorption spectra of the commonly observed spectral bands to compare the differences in spectral line splitting and intensities.

Emission Spectroscopy

Raw spectra

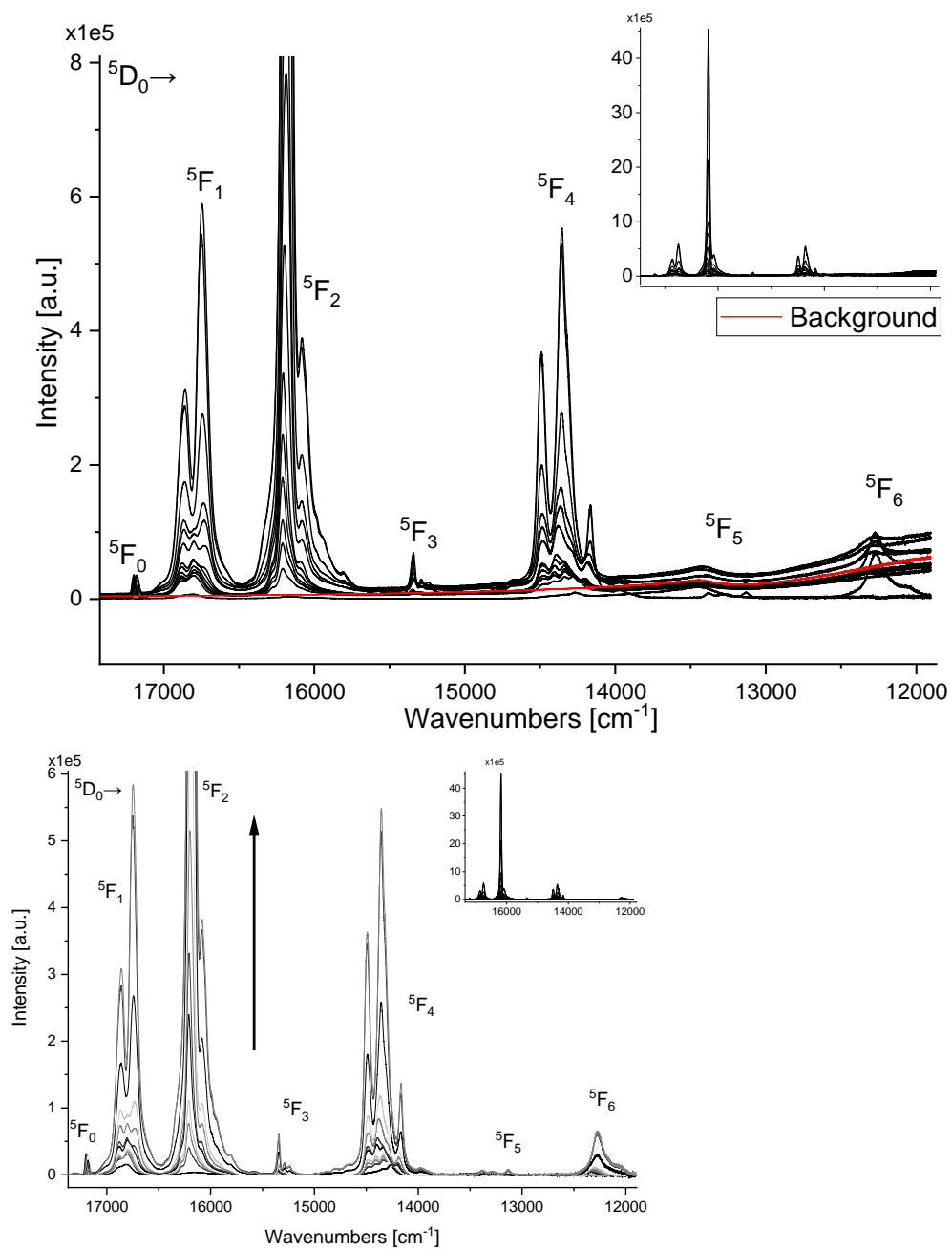


Figure S17 – Left: Raw emission spectra of the europium(III) DPA titration series. The red line shows a dark measurement with closed slits to indicate the background. Right: Background corrected spectra of the titration series.

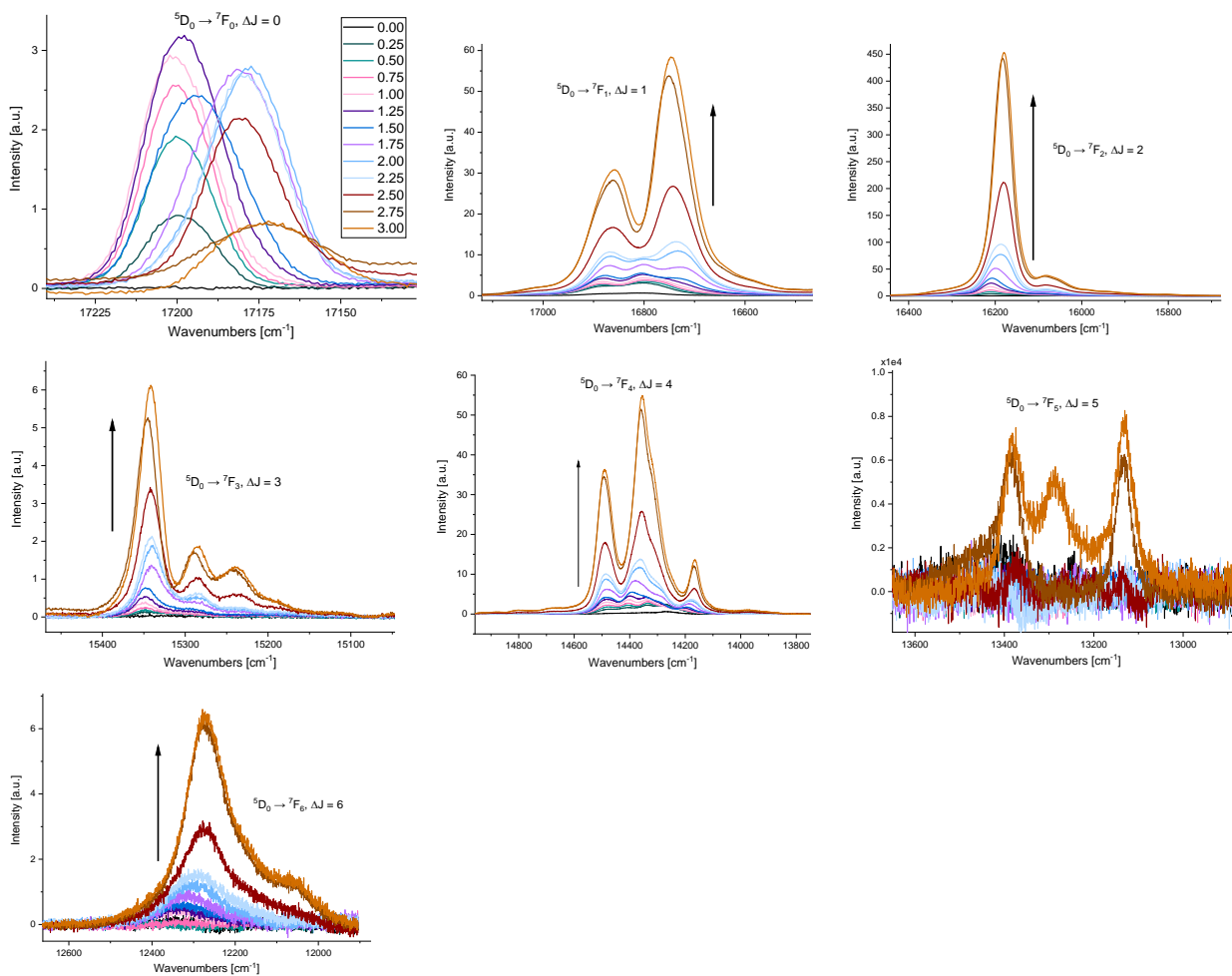


Figure S18 – Emission spectra of the background corrected transitions from the 5D_0 emissive state.

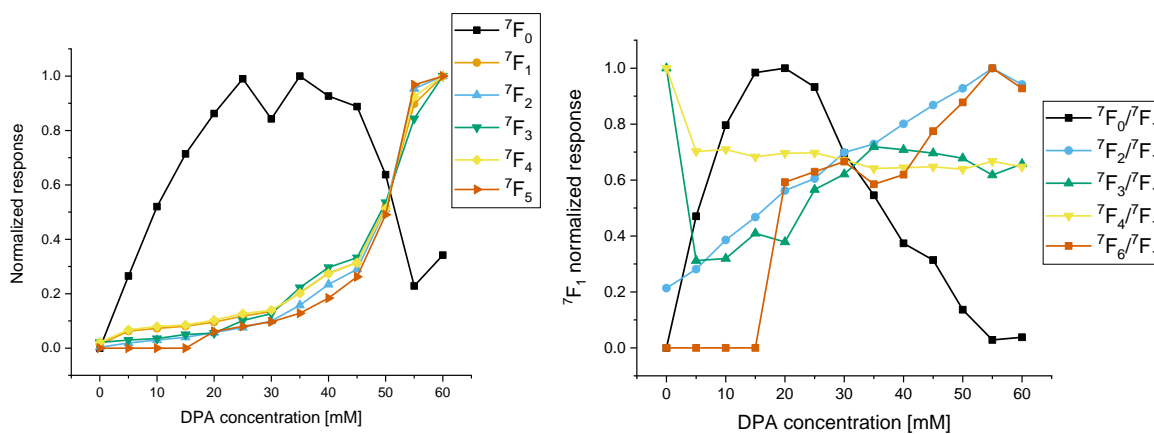


Figure S19 – Isotherms of the emission band areas. Left: Raw emission responses of each band. Right: Intensive responses, normalized by the 7F_1 emission band area.

Spectra normalized by excitation band and τ_{H_2O}

Normalization by τ changes

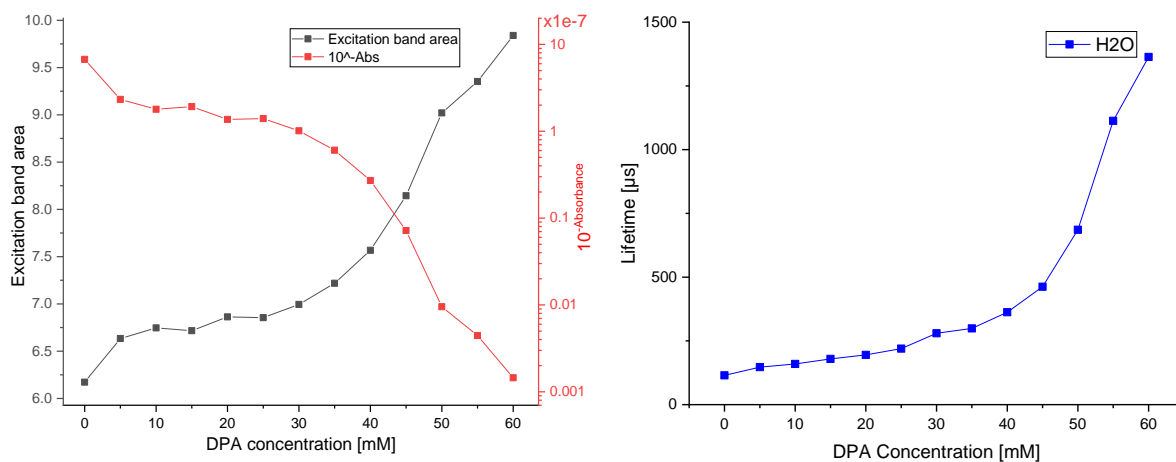


Figure S20 – Left: Absorbance variations in the excitation band. Right: Lifetime isotherms of europium(III) DPA complexes in water. These are used for correcting the emission band intensities to produce A_{rel} to highlight the features of intensive effects on the transition probabilities.

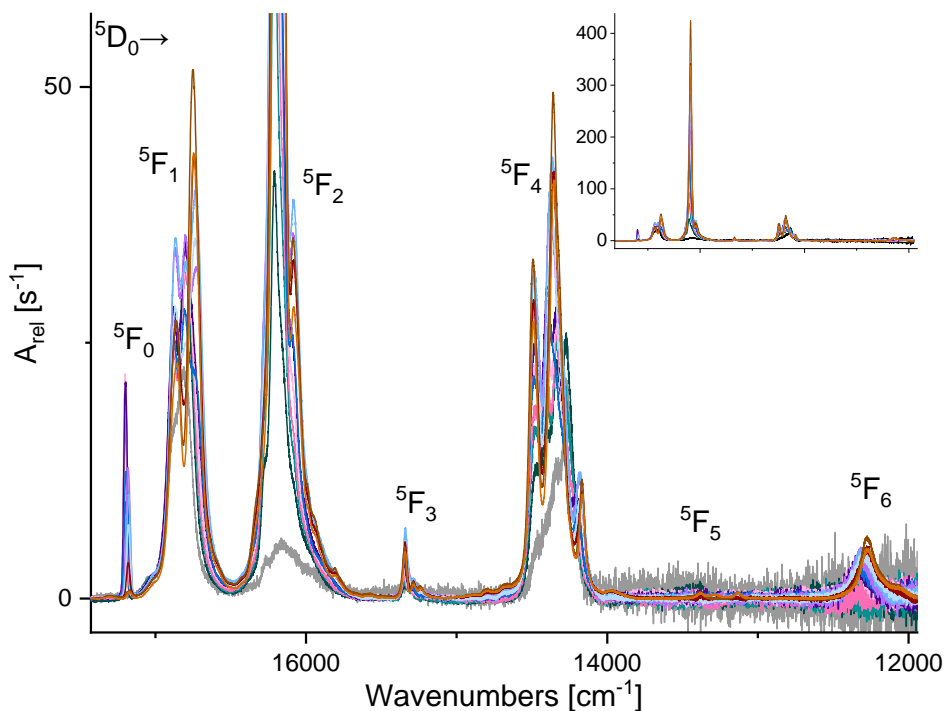


Figure S21 – Emission spectrum corrected by background, excitation band width and lifetimes in H_2O .

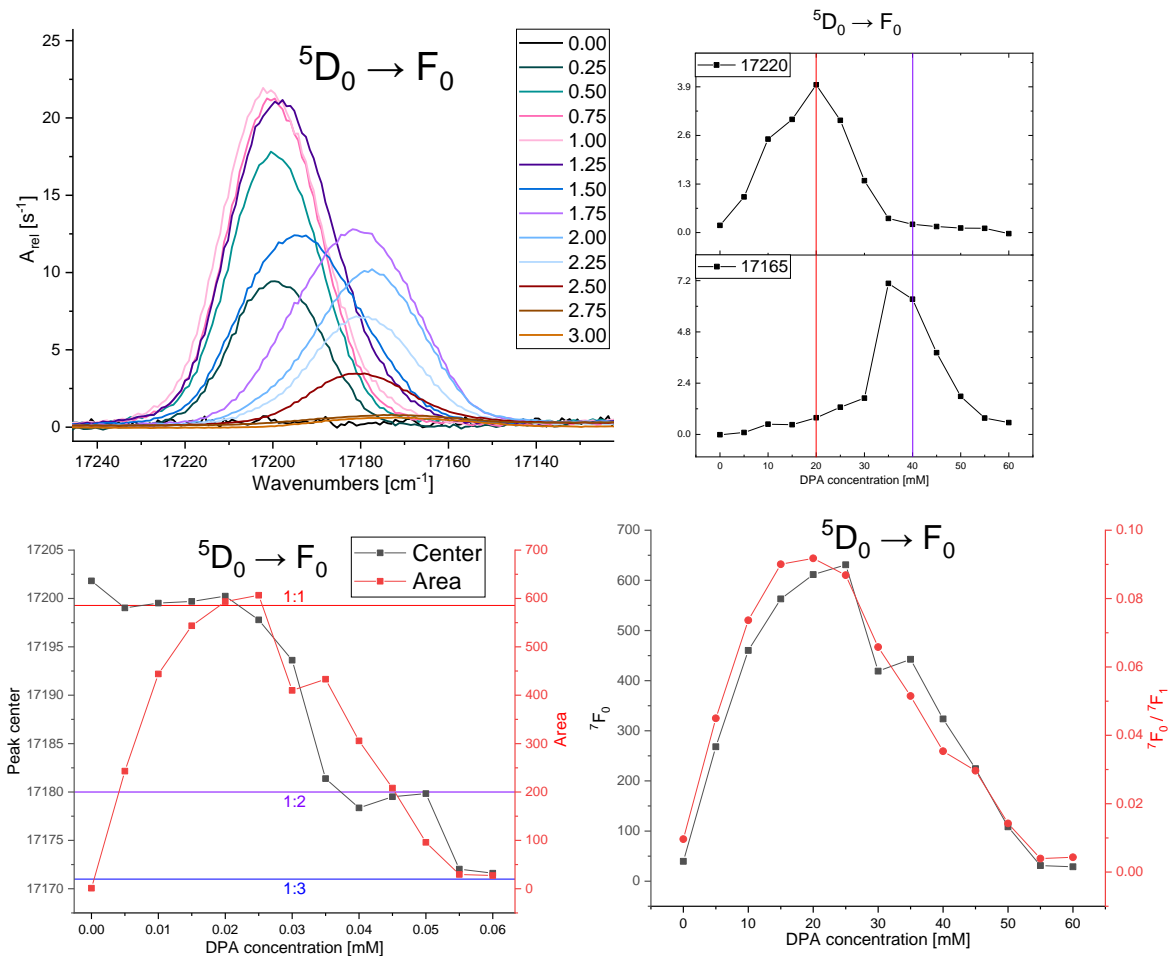


Figure S22 – Emission of the corrected ${}^5D_0 \rightarrow {}^7F_0$ band, the isotherms of selected energies, peak center and peak area both directly and normalized by 7F_1 .

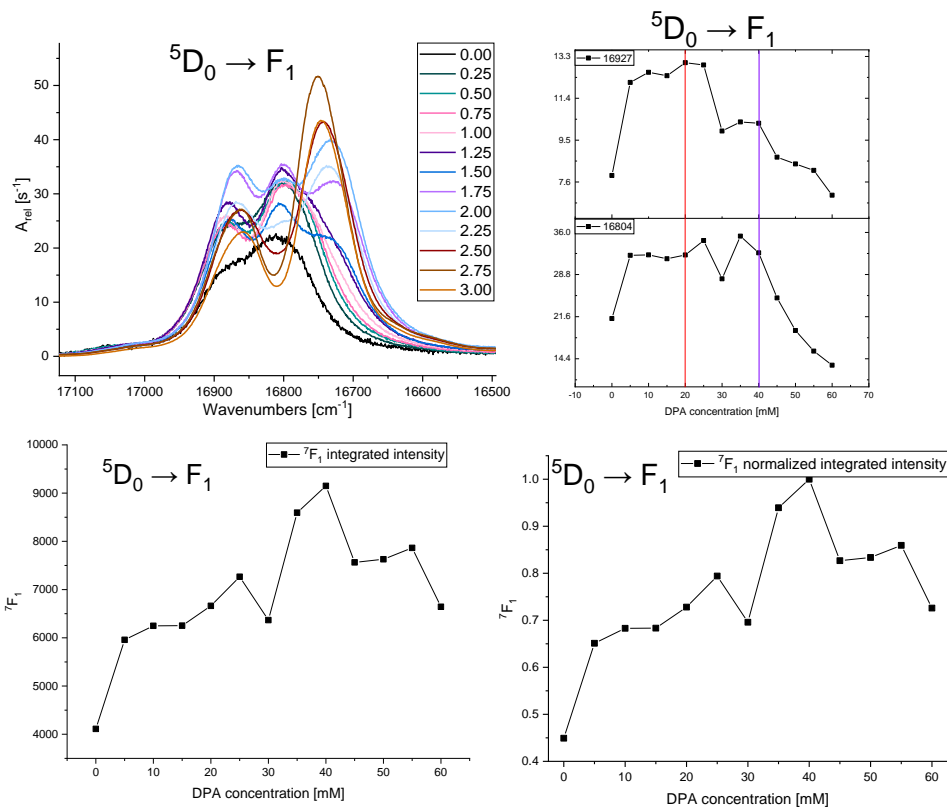


Figure S23 - Emission of the corrected ${}^5D_0 \rightarrow {}^7F_1$ band, the isotherms of selected energies and the band intensity both raw and normalized.

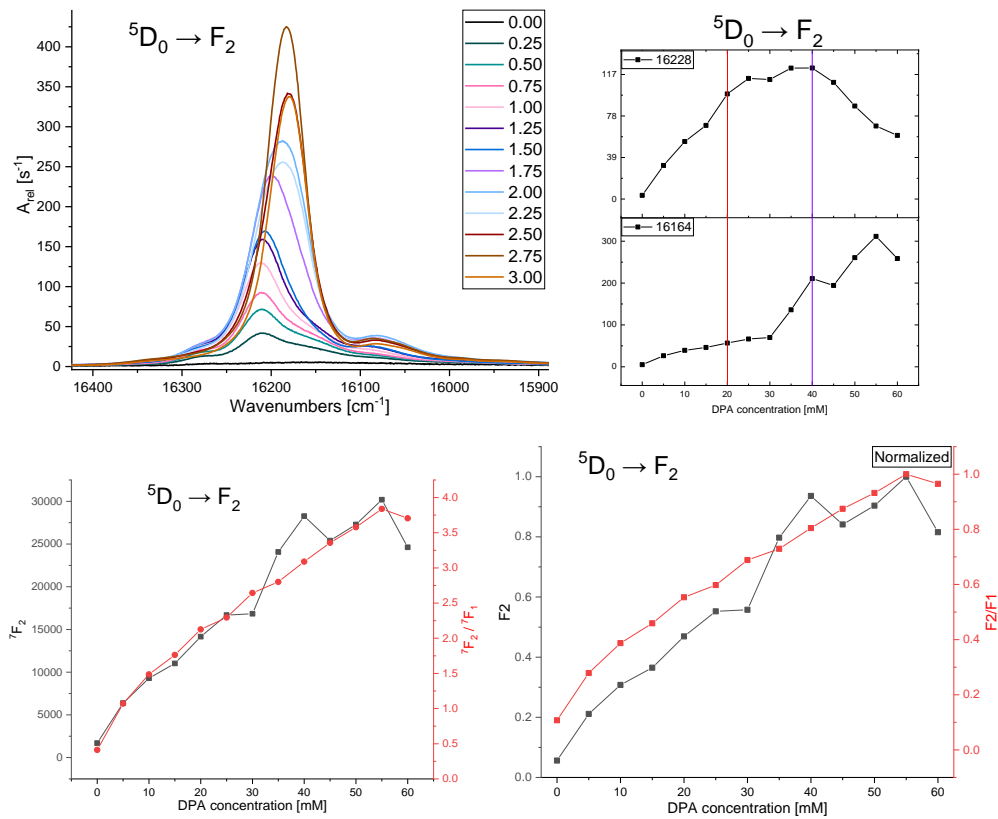


Figure S24 - Emission of the corrected ${}^5D_0 \rightarrow {}^7F_2$ band, the isotherms of selected energies, peak center and peak area both directly and normalized by 7F_1 .

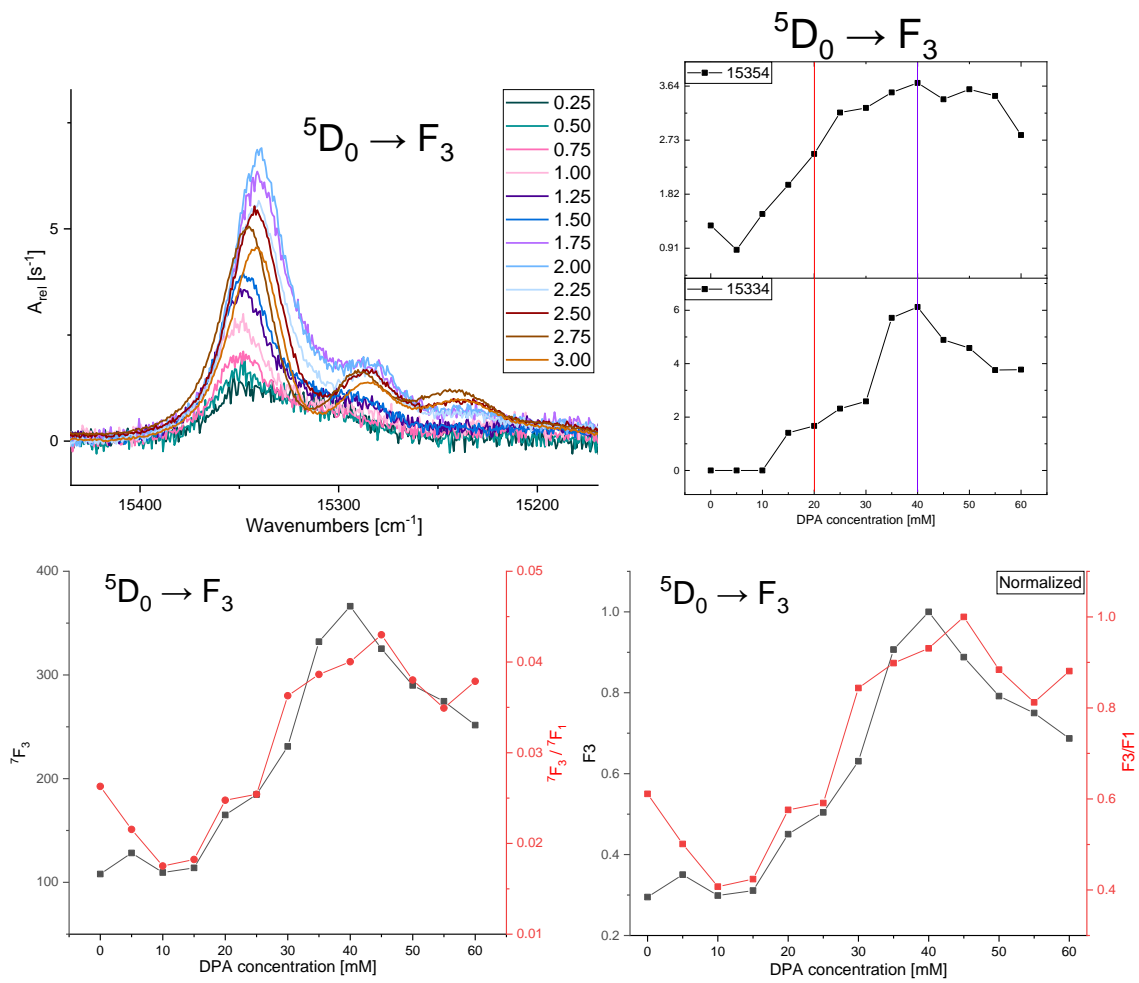


Figure S25 - Emission of the corrected ${}^5D_0 \rightarrow {}^7F_3$ band, the isotherms of selected energies, peak center and peak area both directly and normalized by 7F_1 .

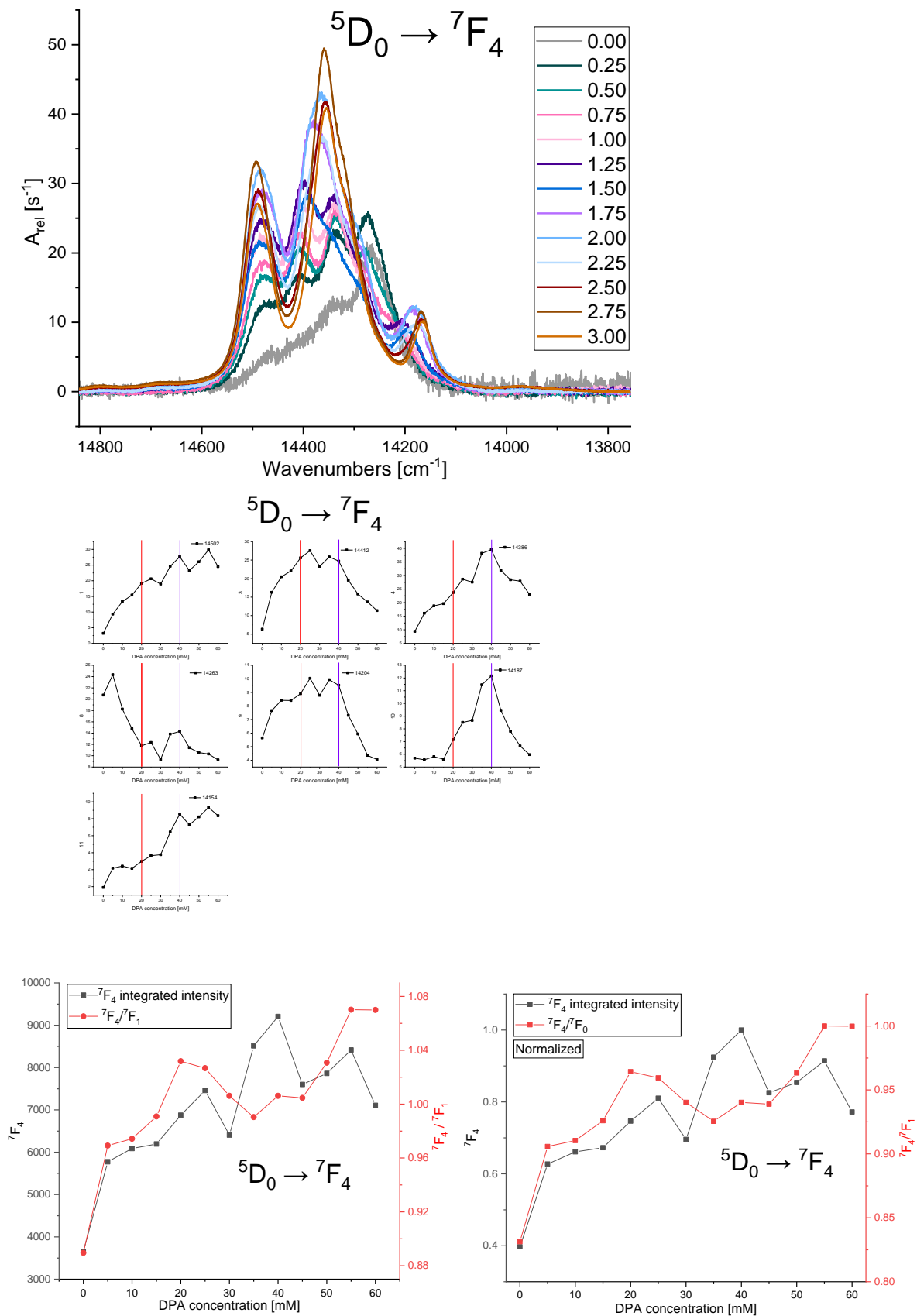


Figure S26 - Emission of the corrected ${}^5D_0 \rightarrow {}^7F_4$ band, the isotherms of selected energies and peak area both direct and normalized by 7F_1 .

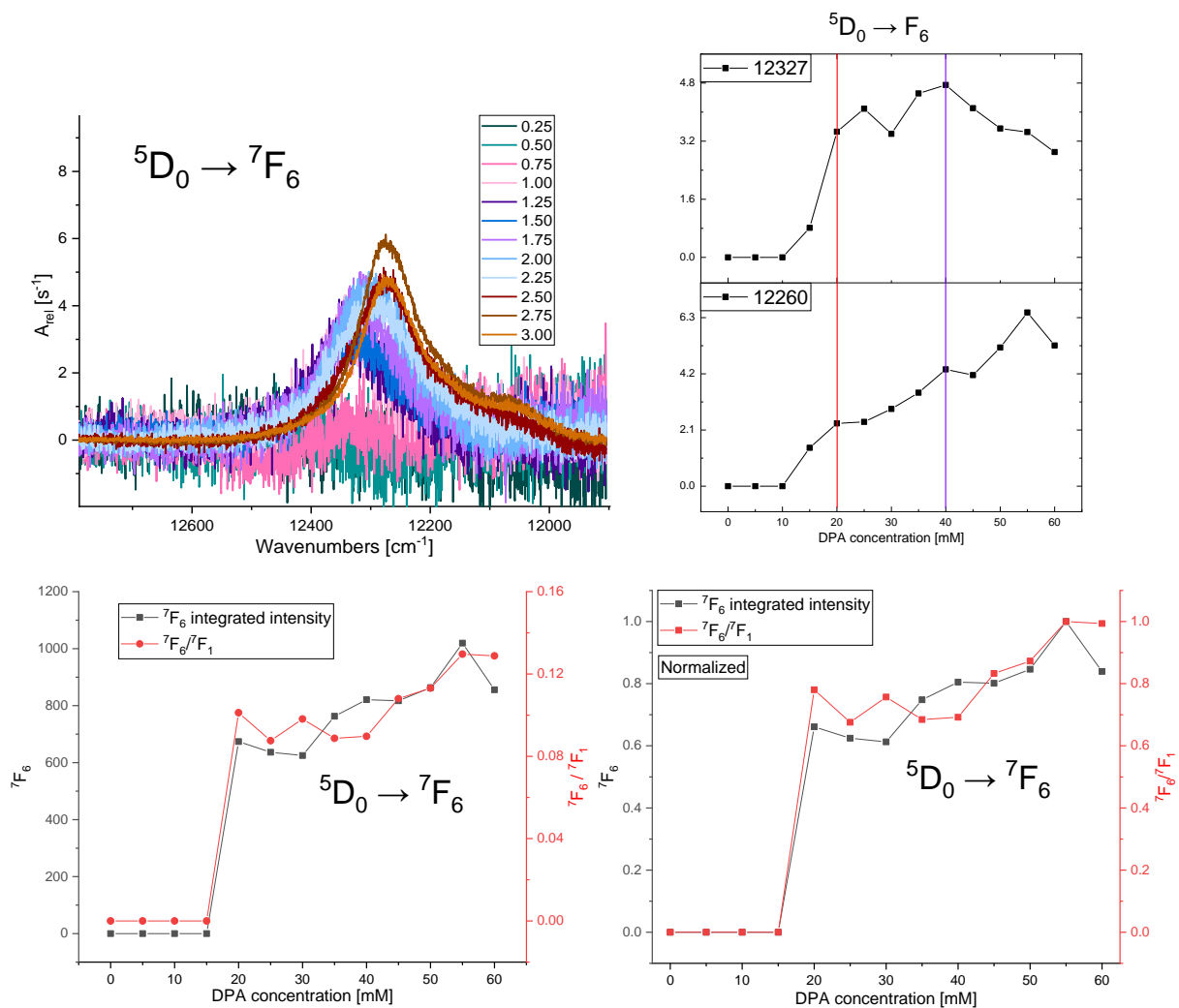


Figure S27 - Emission of the corrected ${}^5D_0 \rightarrow {}^7F_6$ band, the isotherms of selected energies and peak area both direct and normalized by 7F_1 .

Spectroscopy Isotherms

Absorption

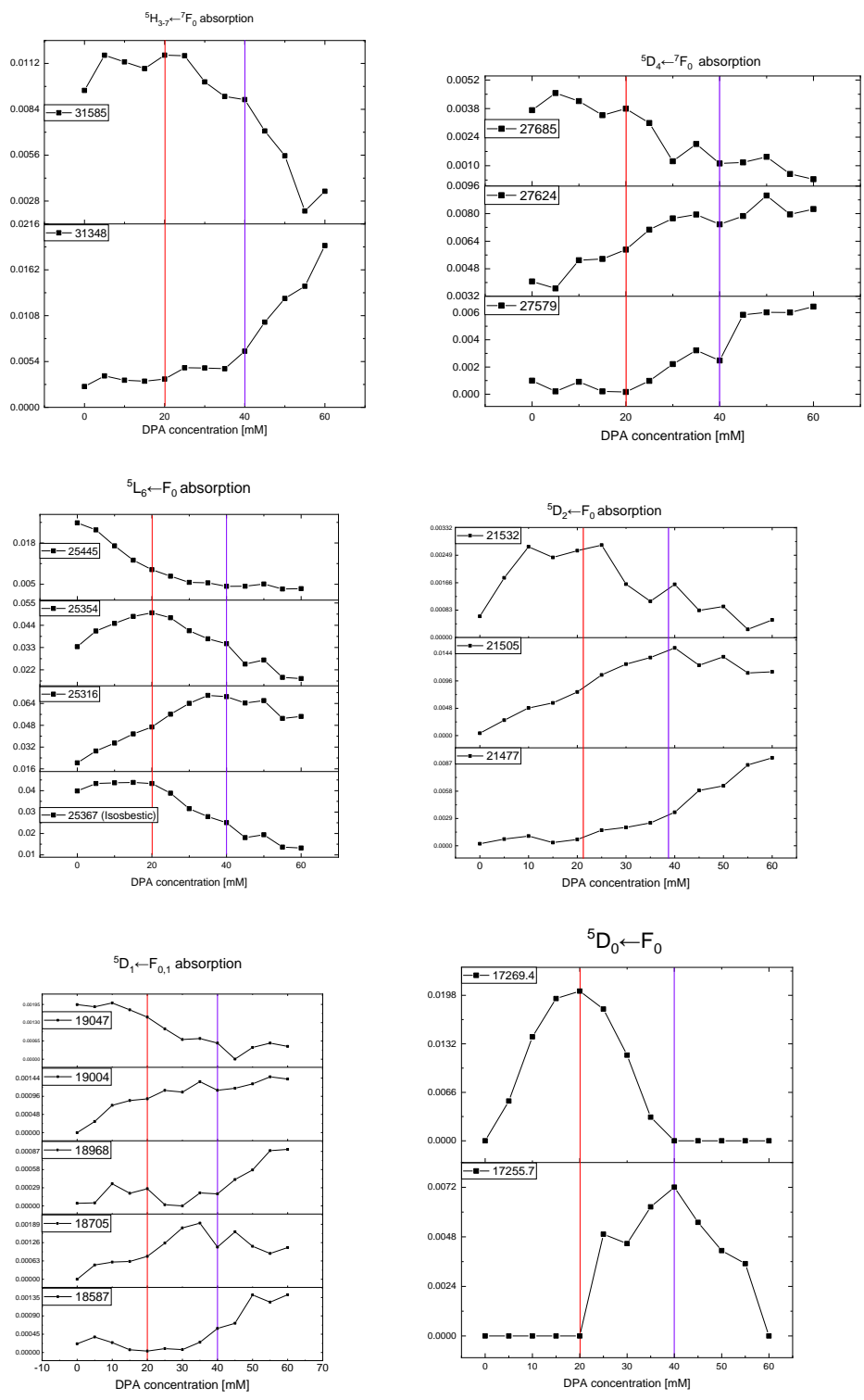


Figure S28 – Intensity isotherms at chosen energies for several absorption bands illustrating the change in line intensity with increasing [DPA].

Excitation

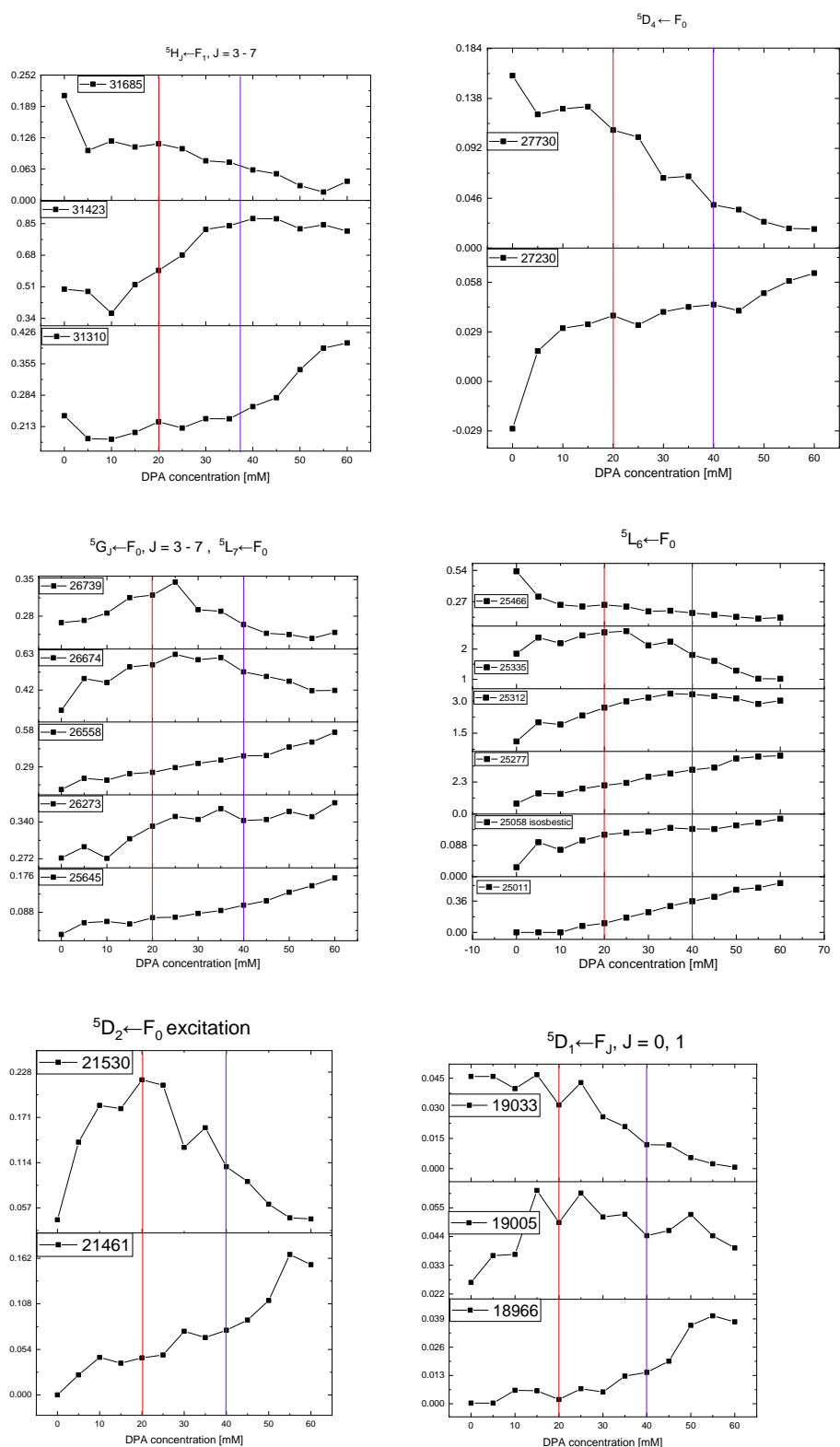


Figure S29 - Intensity isotherms at chosen energies for several excitation bands illustrating the change in line intensity with increasing [DPA]. Isotherms are taken from corrected excitation spectra corrected for coordination sphere hydration and variations in emission intensity.

Emission

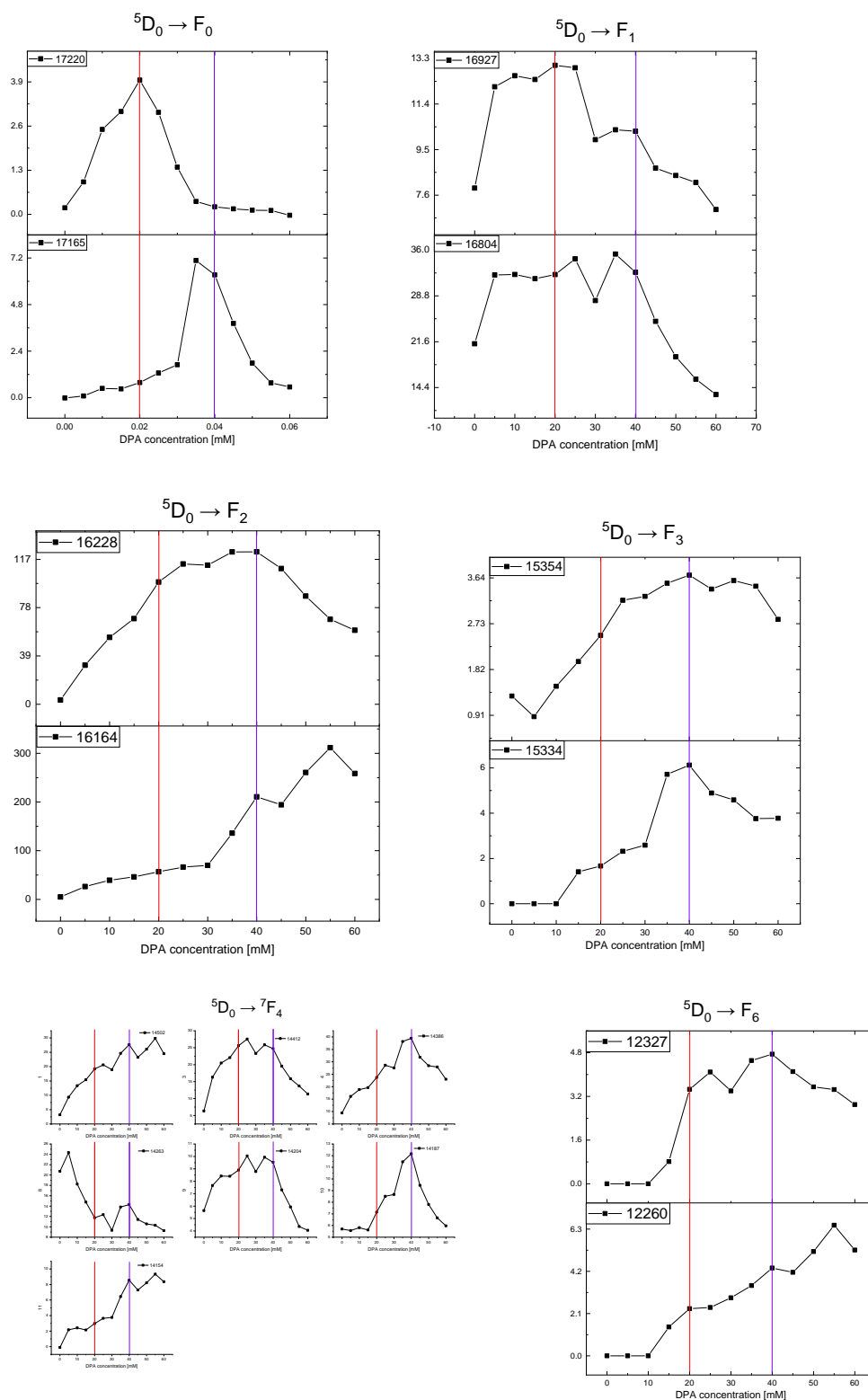


Figure S30 - Intensity isotherms at chosen energies for several emission bands illustrating the change in line intensity with increasing [DPA]. Isotherms are taken from corrected emission spectra corrected for coordination sphere hydration and variations in excitation band intensity.

NMR Spectroscopy

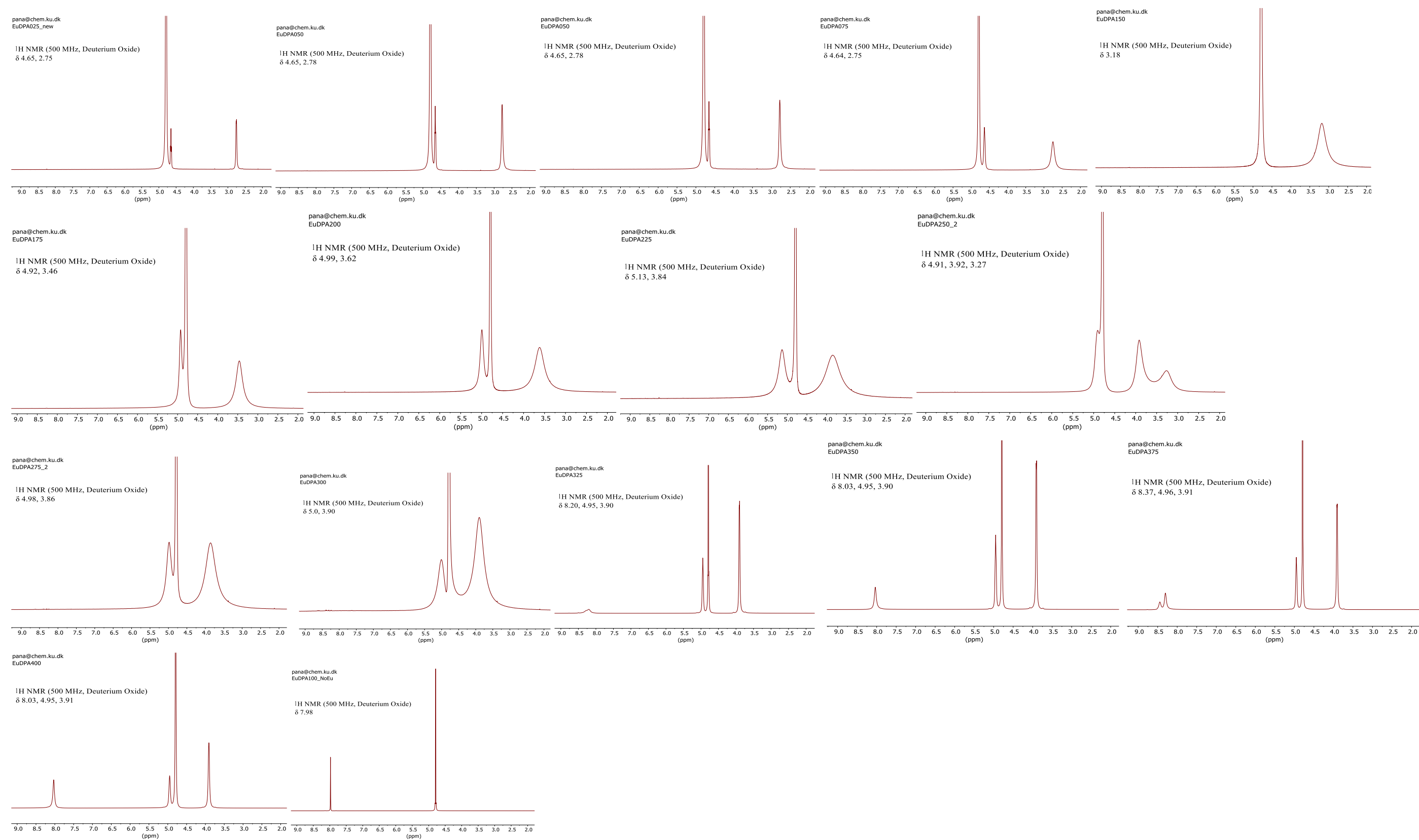


Figure S31 – ^1H NMR of the individual spectra of the europium(III) DPA titration series. The DPA equivalents of each spectrum is imposed in the plots as Eu:DPA 100:xxx.

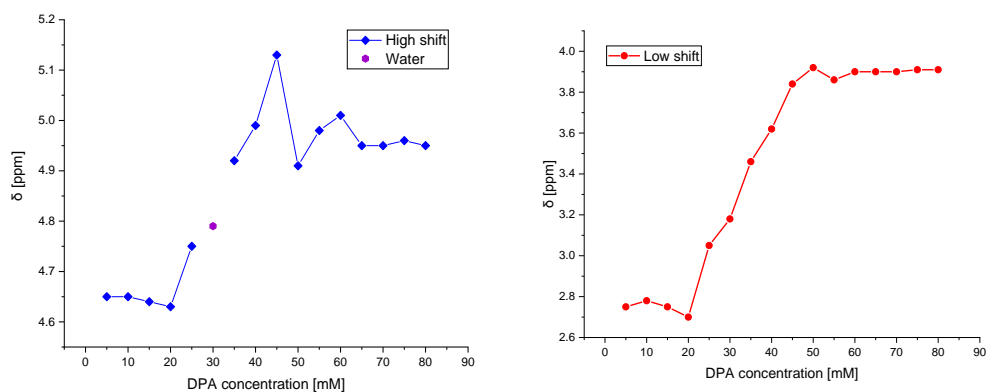
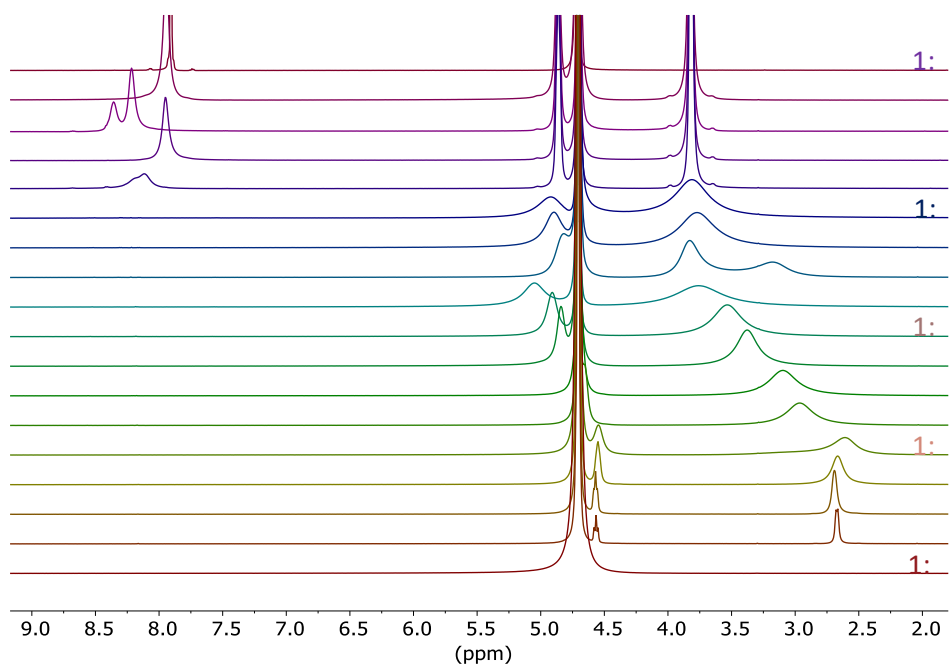


Figure 32 – Top: Stacked ^1H NMR spectra of the europium(III) DPA titration series. Bottom: Isotherms of the high and low shifted proton signal of the ^1H NMR spectra shown in Figure 31.

Total Scattering – Pair Distribution Functions

I(Q)

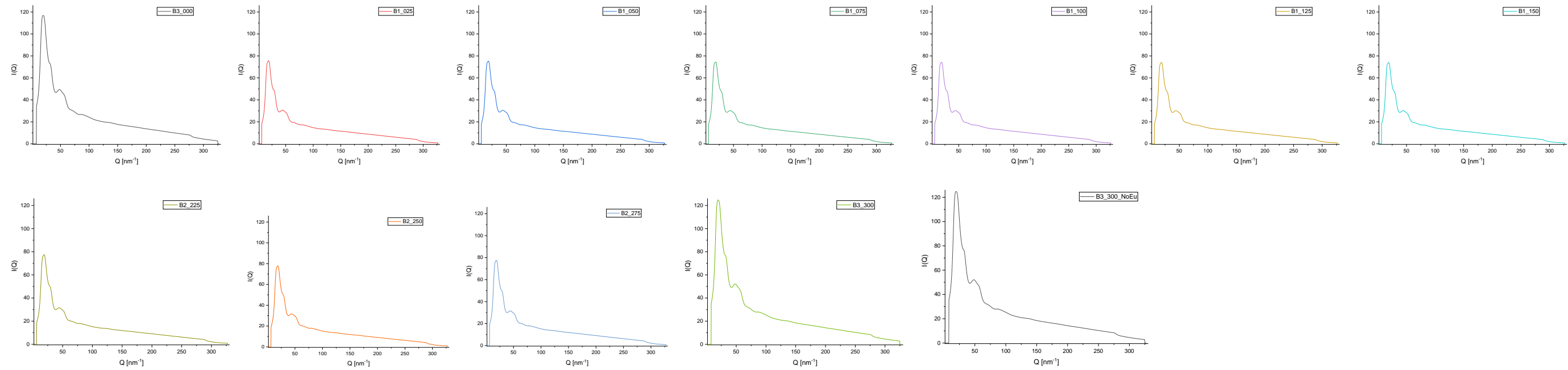
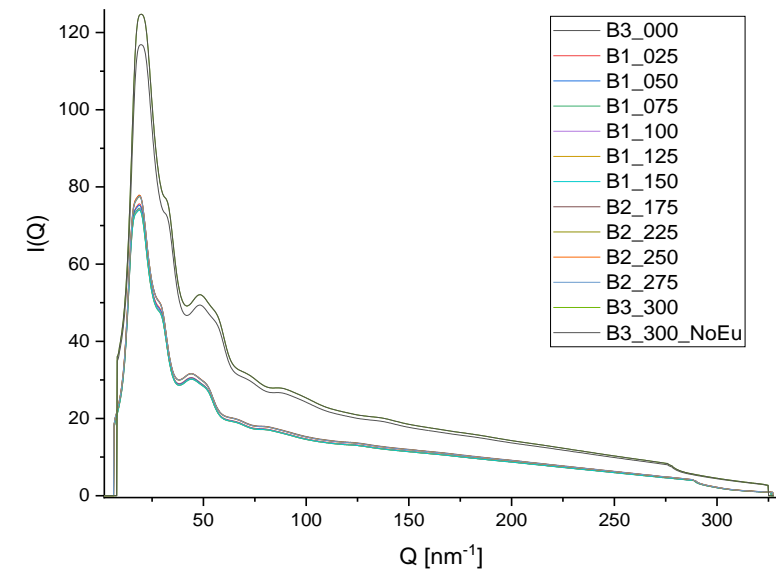


Figure S33 – I(Q) 1D diffraction patterns of the europium(III) DPA titration series. Data was collected over three batches, BX, X = 1-3. Eu:DPA ratios of each samples are imposed on the plots as 100:xxx.

F(Q)

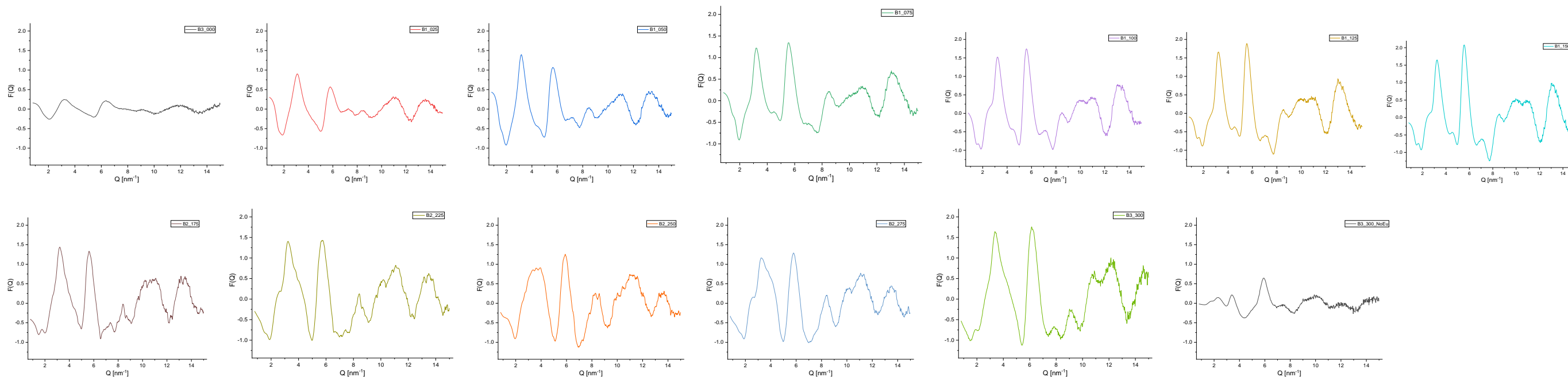
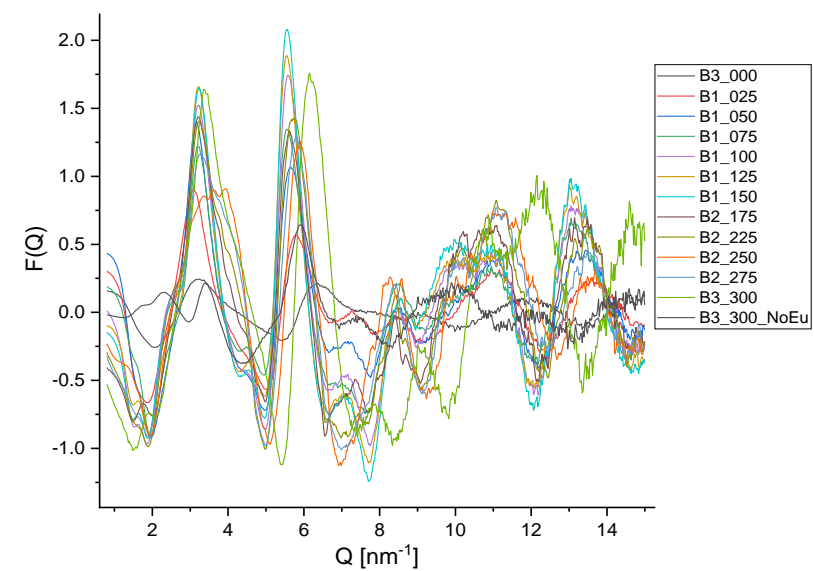


Figure S34 – F(Q) of the europium(III) DPA titration series. Data was collected over three batches, BX, X = 1-3. Eu:DPA ratios of each samples are imposed on the plots as 100:xxx.

$S(Q)$

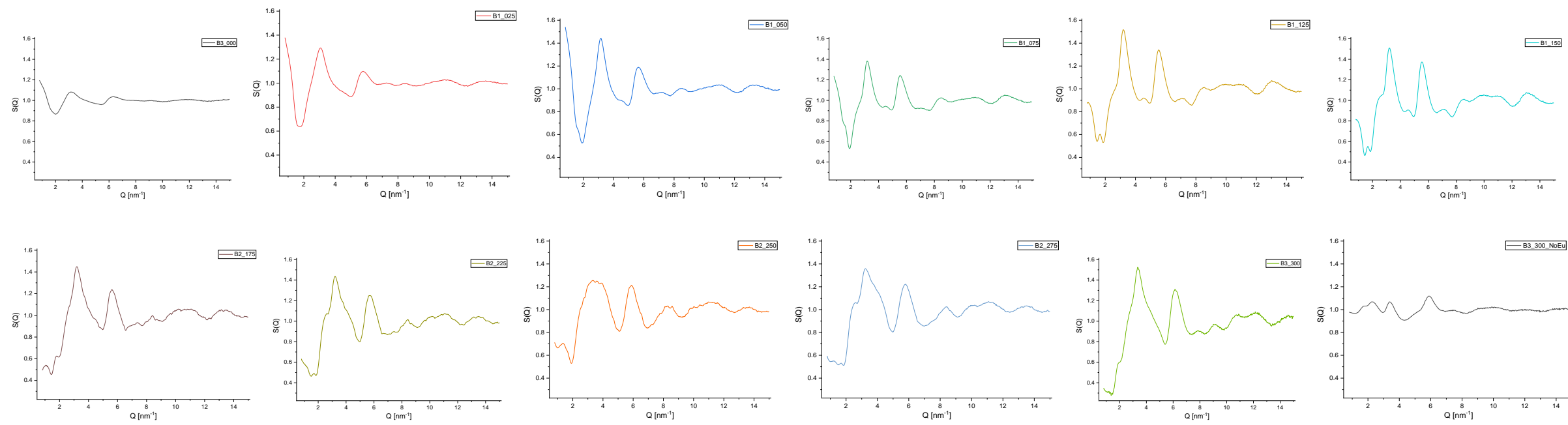
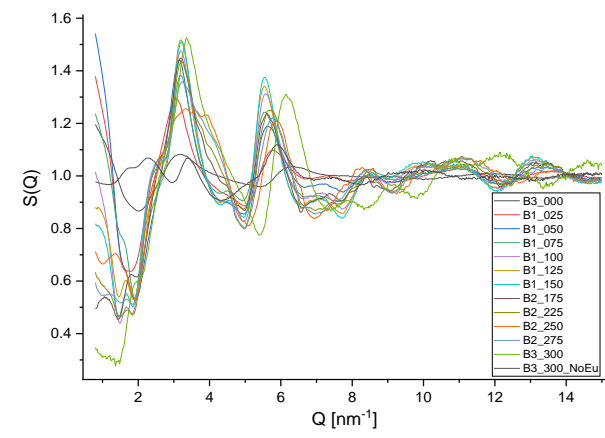


Figure S35 – $S(Q)$ of the europium(III) DPA titration series. Data was collected over three batches, BX, X = 1-3. Eu:DPA ratios of each samples are imposed on the plots as 100:xxx.

G(r)

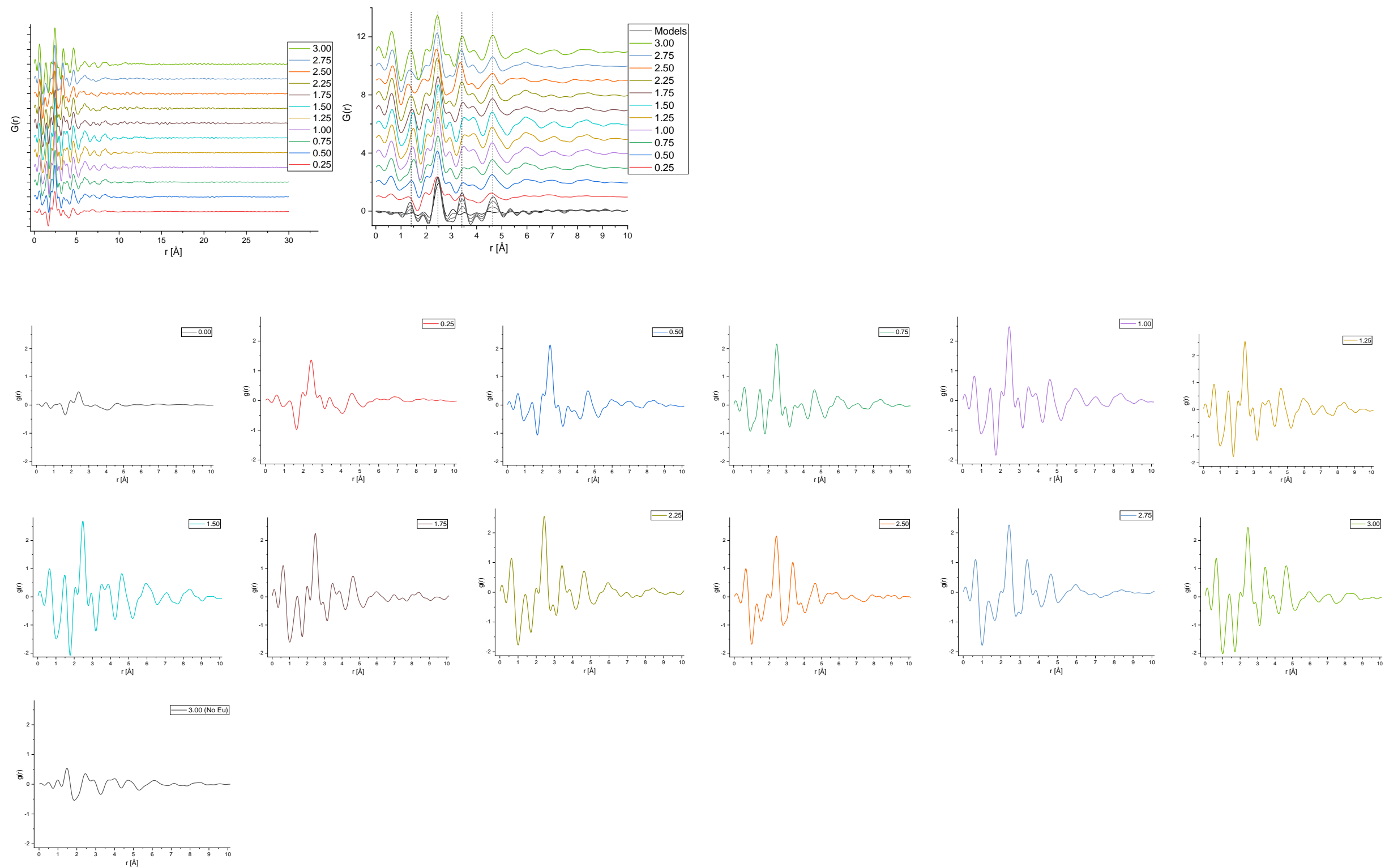


Figure S36 – G(r) of the europium(III) DPA titration series. Data was collected over three batches, BX, X = 1-3. Eu:DPA ratios of each samples are imposed on the plots as 100:xxx.

DynaFit speciation modelling

Absorption spectroscopy

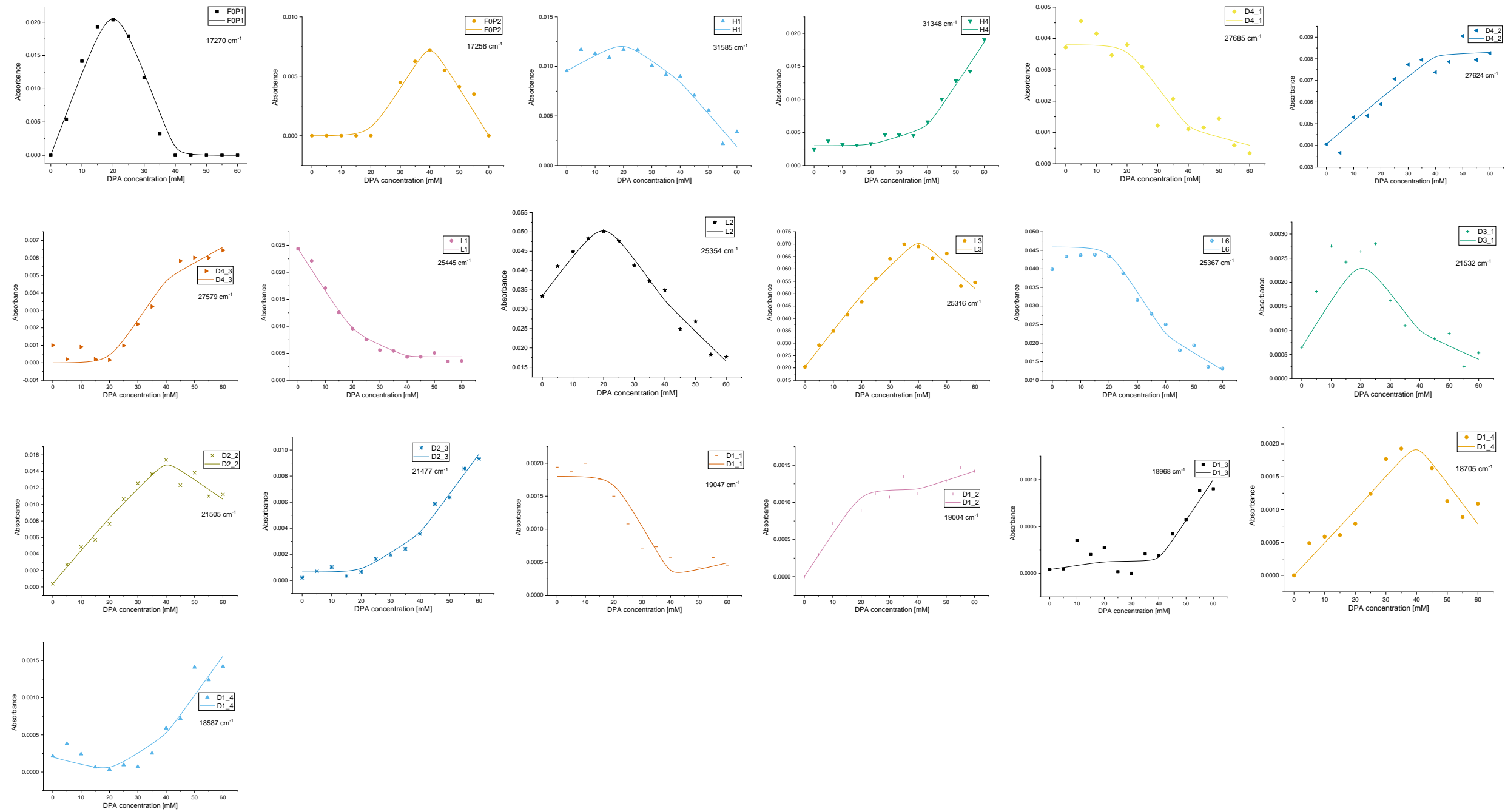


Figure S37 - Models generated in DynaFit describing isotherms of absorbance at specific energies.

Optimized Parameters

| No. | Par#Set | Initial | Final | Std. Error | CV (%) | Low ^(a) | High ^(a) | Note |
|-----|---------|----------|-----------------|------------|--------|--------------------|---------------------|------|
| #1 | K1 | 5e+011 | 3.8e+011 | 6e+011 | 157.0 | 2.2e+011 | 7.1e+011 | |
| #2 | K2 | 5e+009 | 5e+009 | 7.8e+009 | 156.0 | 2.6e+009 | 8.4e+009 | |
| #3 | K3 | 1.6e+007 | 1.7e+007 | 2.9e+007 | 168.5 | 2.7e+006 | 4.4e+007 | |

^(a) Confidence intervals at **95 %** probability level.

100 × Correlation Matrix

| No. | Par#Set | #1 | #2 | #3 |
|-----|---------|----|----|----|
| #1 | K1 | * | 98 | 89 |
| #2 | K2 | 98 | * | 91 |
| #3 | K3 | 89 | 91 | * |

Confidence Interval Profiles

Confidence interval for K1, K2, K3

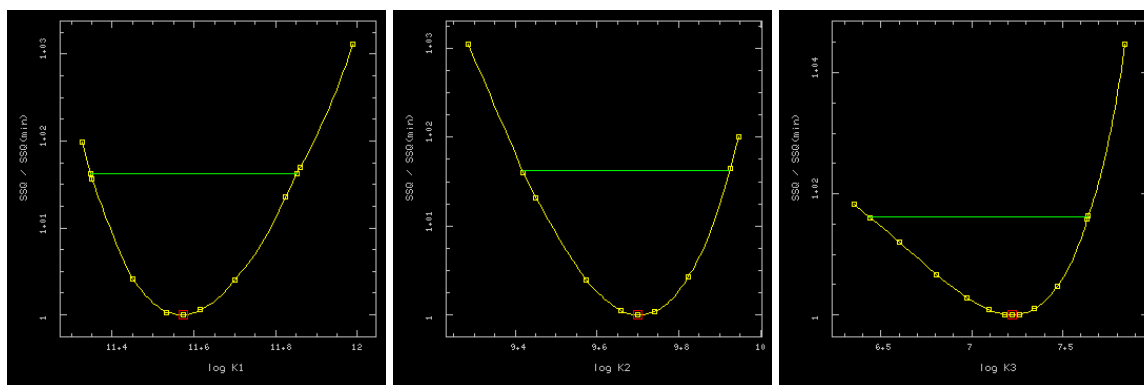


Figure S38 – Confidence intervals for the fits of the binding constants of the three equilibria in the europium(III) DPA model system, generated from the absorption isotherms.

Absorption speciation

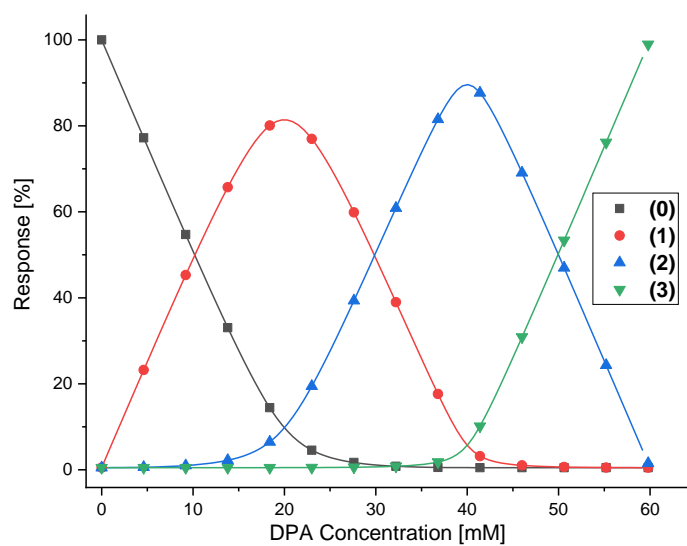


Figure S39 – Speciation plot that illustrate the molar fractions of the four europium(III) DPA complexes for a given DPA concentration.

Table S2 – Concentrations and molar fractions of the four europium(III) species in solution, based on the values of the normalized speciation model ().

| Calc. Speciation | (0) | (1) | (2) | (3) |
|------------------|--------------------|---------------|---------------|---------------|
| 0 | [mM] 20.00 | - | - | - |
| | Mol% 100 % | - | - | - |
| 5 | [mM] 15.2 | 5.0 | - | - |
| | Mol% 75.1 % | 24.8 % | 0.1 % | - |
| 10 | [mM] 10.1 | 9.8 | 0.1 | - |
| | Mol% 50.6 % | 48.8 % | 0.6 % | - |
| 15 | [mM] 5.5 | 14.0 | 0.5 | - |
| | Mol% 27.4 % | 70.3 % | 2.3 % | - |
| 20 | [mM] 1.9 | 16.3 | 1.9 | - |
| | Mol% 9.3 % | 81.3 % | 9.3 % | - |
| 25 | [mM] 0.5 | 14.1 | 5.5 | - |
| | Mol% 2.4 % | 70.3 % | 27.3 % | - |
| 30 | [mM] 0.1 | 9.8 | 10.1 | - |
| | Mol% 0.6 % | 48.9 % | 50.3 % | 0.2 % |
| 35 | [mM] - | 5.1 | 14.8 | 0.1 |
| | Mol% 0.1 % | 25.5 % | 73.7 % | 0.7 % |
| 40 | [mM] - | 1.0 | 17.9 | 1.1 |
| | Mol% - | 5.2 % | 89.6 % | 5.2 % |
| 45 | [mM] - | 0.1 | 14.7 | 5.1 |
| | Mol% - | 0.7 % | 73.6 % | 25.7 % |
| 50 | [mM] - | - | 9.9 | 10.0 |
| | Mol% - | 0.2 % | 49.7 % | 50.2 % |
| 55 | [mM] - | - | 4.9 | 15.0 |
| | Mol% - | - | 24.9 % | 75.0 % |
| 60 | [mM] - | - | - | 19.9 |
| | Mol% - | - | 0.2 % | 99.8 % |

Comparison of speciation model with emission isotherms

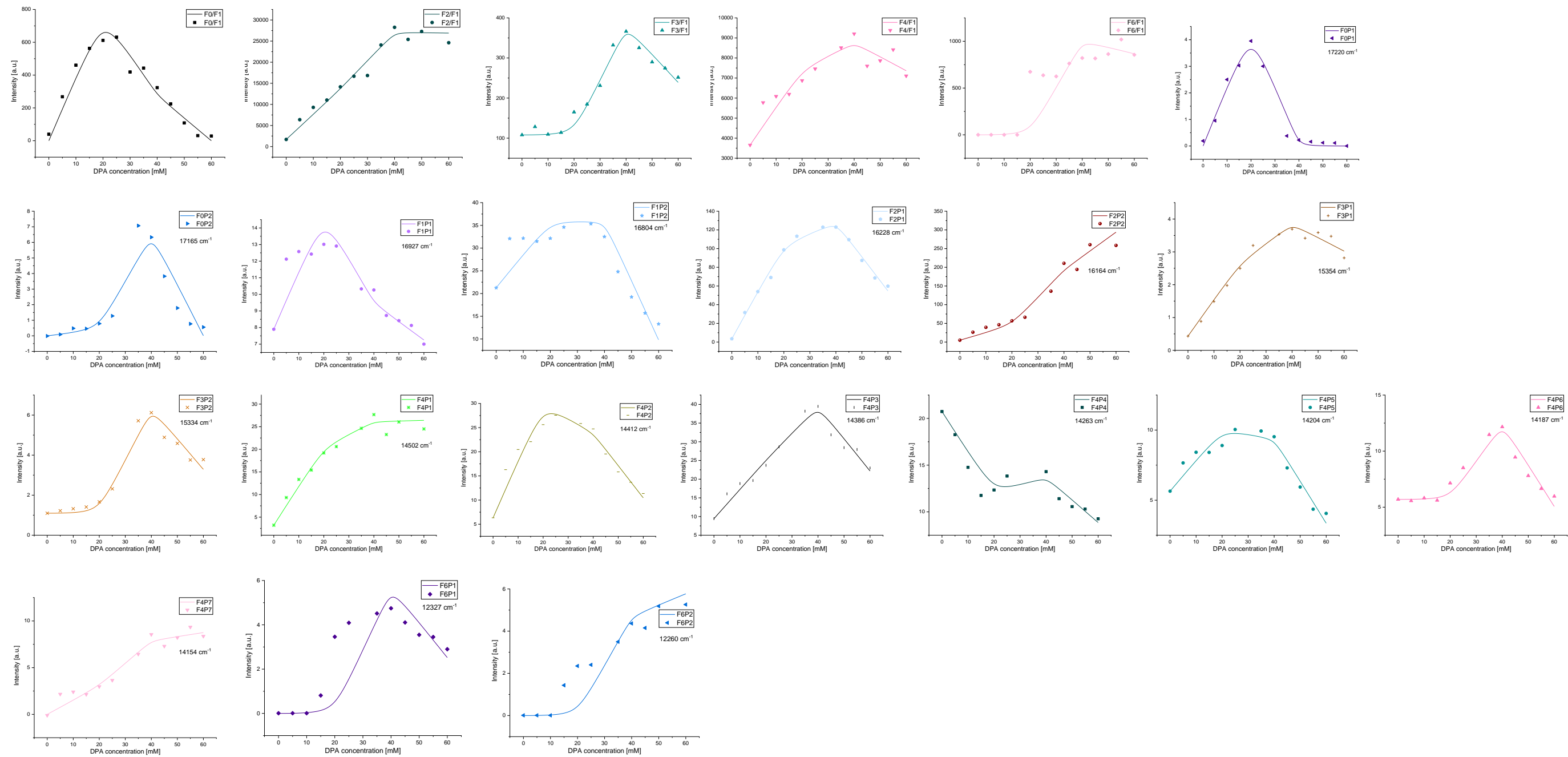


Figure S40 - Models generated in DynaFit describing isotherms of emission intensity at specific energies.

Excitation

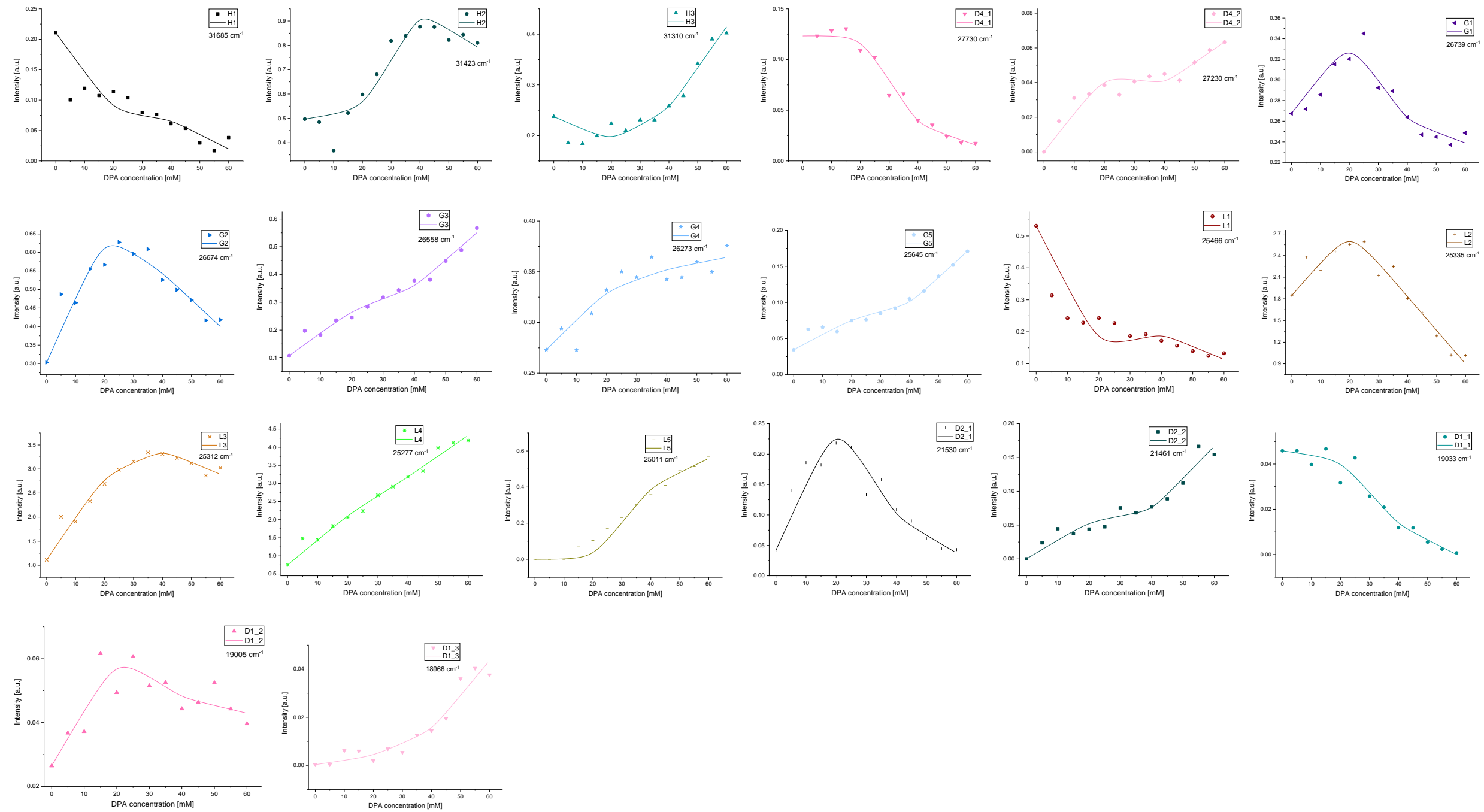


Figure S41 - Models generated in DynaFit describing isotherms of excitation intensity at specific energies.

NMR

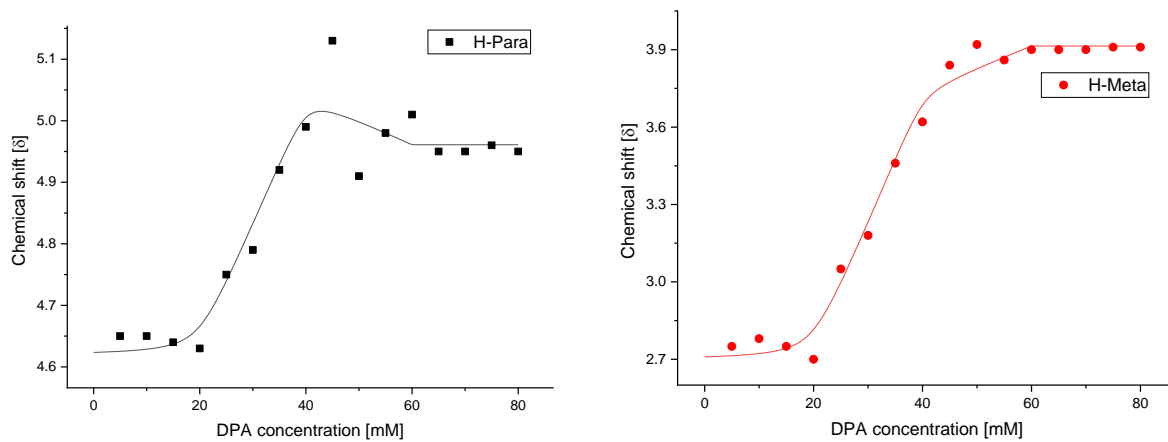


Figure S42 - Models generated in DynaFit describing isotherms of chemical shifts of ^1H NMR spectroscopy for two non-equivalent protons.

Lifetimes & q

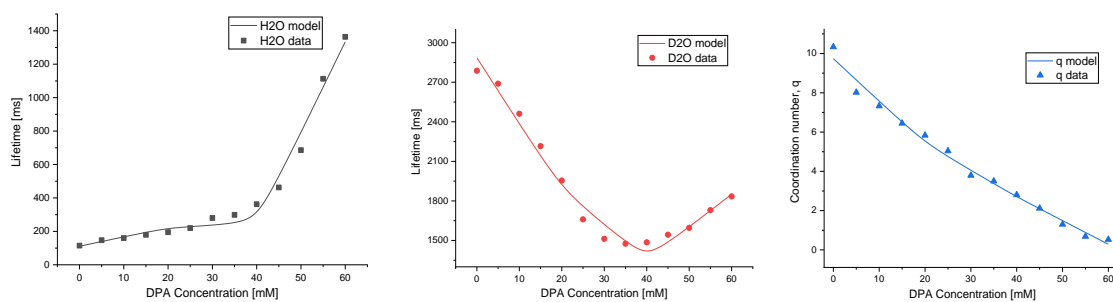


Figure S43 - Models generated in DynaFit describing isotherms of excited state lifetimes in H₂O D₂O and of q.

X-ray scattering data and models from speciation

EuDPA structures and modelled PDF's at varying q

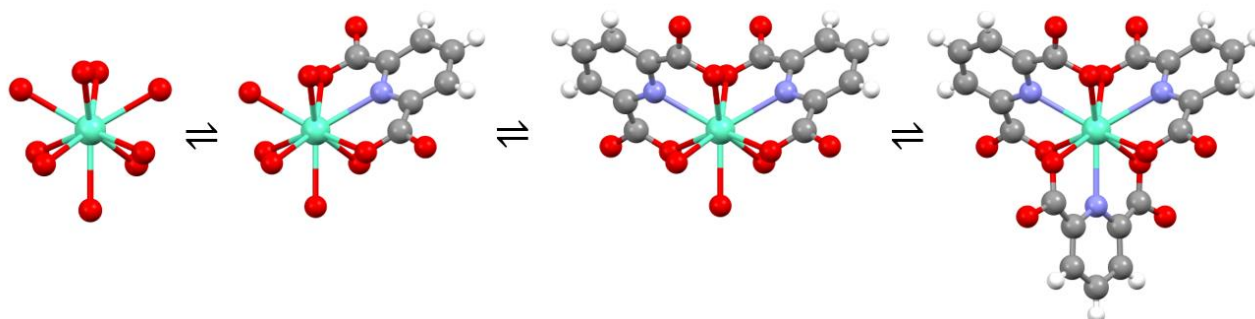


Figure S44 – Crystal structures of (0), (1), (2) and (3). The hydrogens of the water molecules are omitted for clarity.

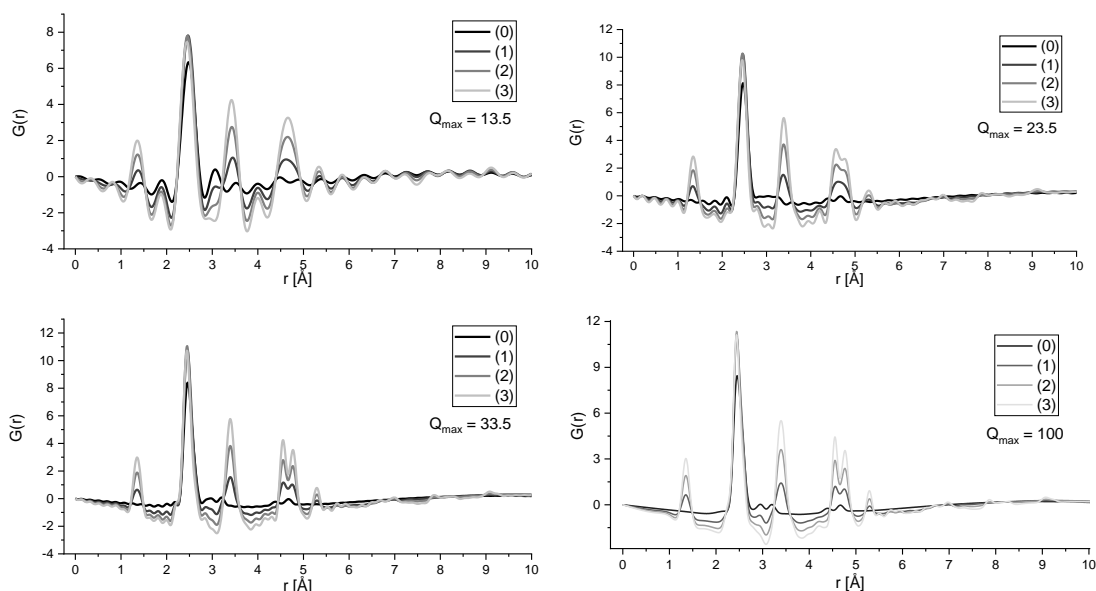


Figure S45 – PDF models calculated from the crystal structures in Figure S44, generated at different values of Q.

Total scattering PDF models and data quality

The structure of $\text{EuDPA}_{3-n}^{+3-2n}$ in solution has been investigated using total x-ray scattering and pair distribution function (PDF) analysis to extract atomic pair distances in the coordination complex that conform to characteristic distances of CSAP or TTP. The scattering profile of a system is collected as the scattering intensity function $I(Q)$, that is converted to the total scattering structure function $S(Q)$ by normalization. This is weighted by the scattering vector Q to produce the reduced total scattering function $F(Q)$ and finally the real-space pair distribution function, $G(r)$ is produced by Fourier transformation. The reader is referred to the book “Underneath the Bragg

peaks” by Takeshi Egami & Simon Billinge for a rigorous description of these functions. The data is compared to PDF models of the coordination complexes shown in figure S45. The comparisons of pair distribution function data and model are shown in figure S46 and S47. Each peak represents a distance in Å where the probability for finding an atomic pair is high and is scaled by the electron density of the scattering pair. The 60 electrons of europium(III) therefore produce strong signals in the scattering data which make atomic pair distances of the europium(III) center easy to distinguish.

Similar to absorption spectroscopy, scattering is an instantaneous process compared to the ligand exchange rate. For this reason, each dataset is compared to linear combinations of the models shown of figure S45 corresponding to the molar fractions derived in Table S2.

To obtain high quality scattering data to high Q, data were collected at the Advanced Photon Source. The range of Q is important, as it signifies how much of Q-space is included in the Fourier Transform and therefore how well the peaks are defined in real-space as well as the resolution of satellite peaks as a consequence of termination ripples. For treatment of the scattering data it was determined that only a $Q_{\max} = 13.5 \text{ \AA}^{-1}$ could be achieved based on the experimental conditions. The decrease in data quality with increasing Q can be seen from figure S47 where the level of noise become significant above 13.5 \AA^{-1} .

Model and data of EuDPA samples

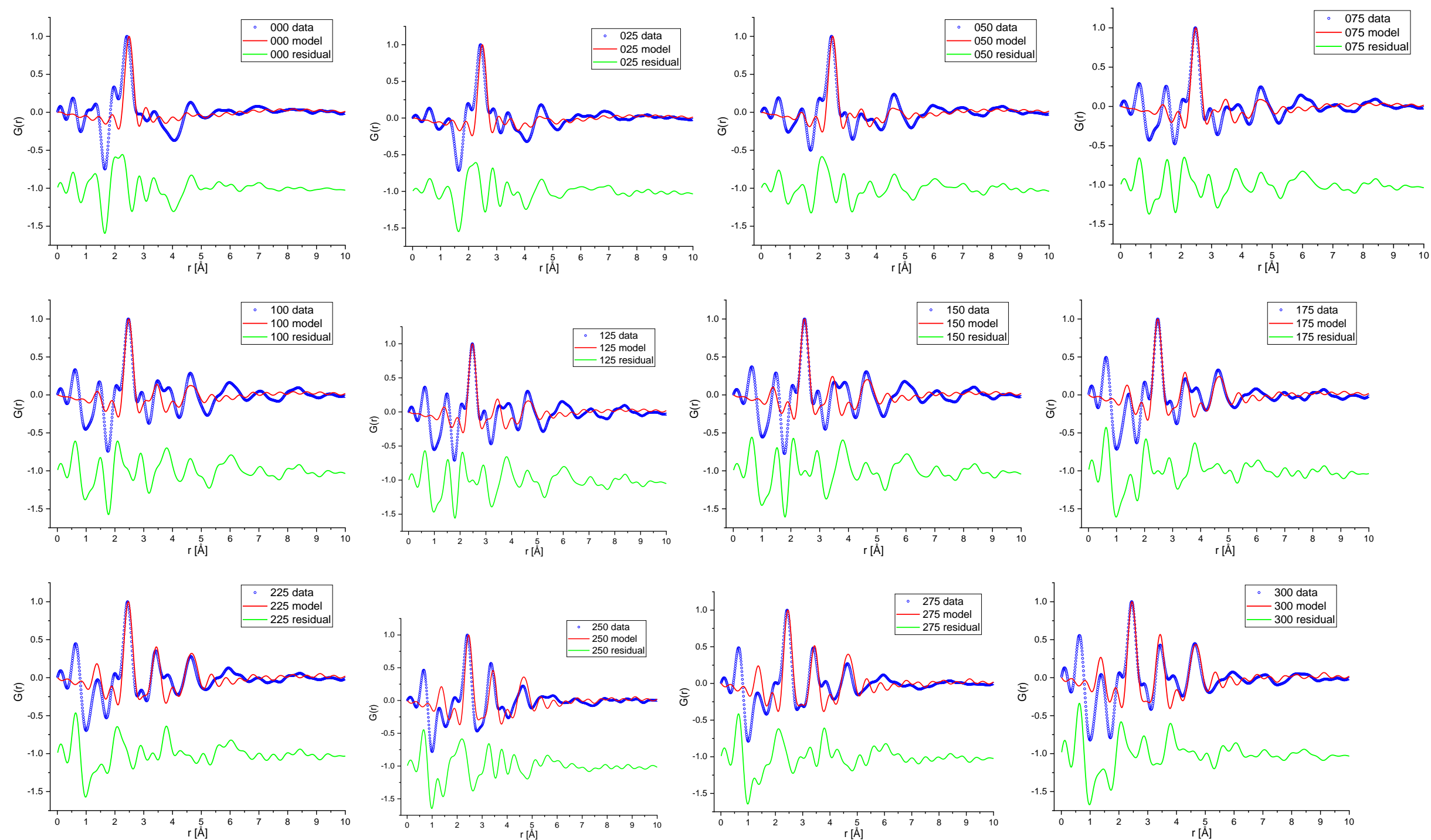


Figure S46 – Data, model and residuals of the europium(III) DPA titration series. Data and models are generated with a $Q_{\max} = 13.5 \text{ \AA}^{-1}$.

Models and fit with $q = 33.5$

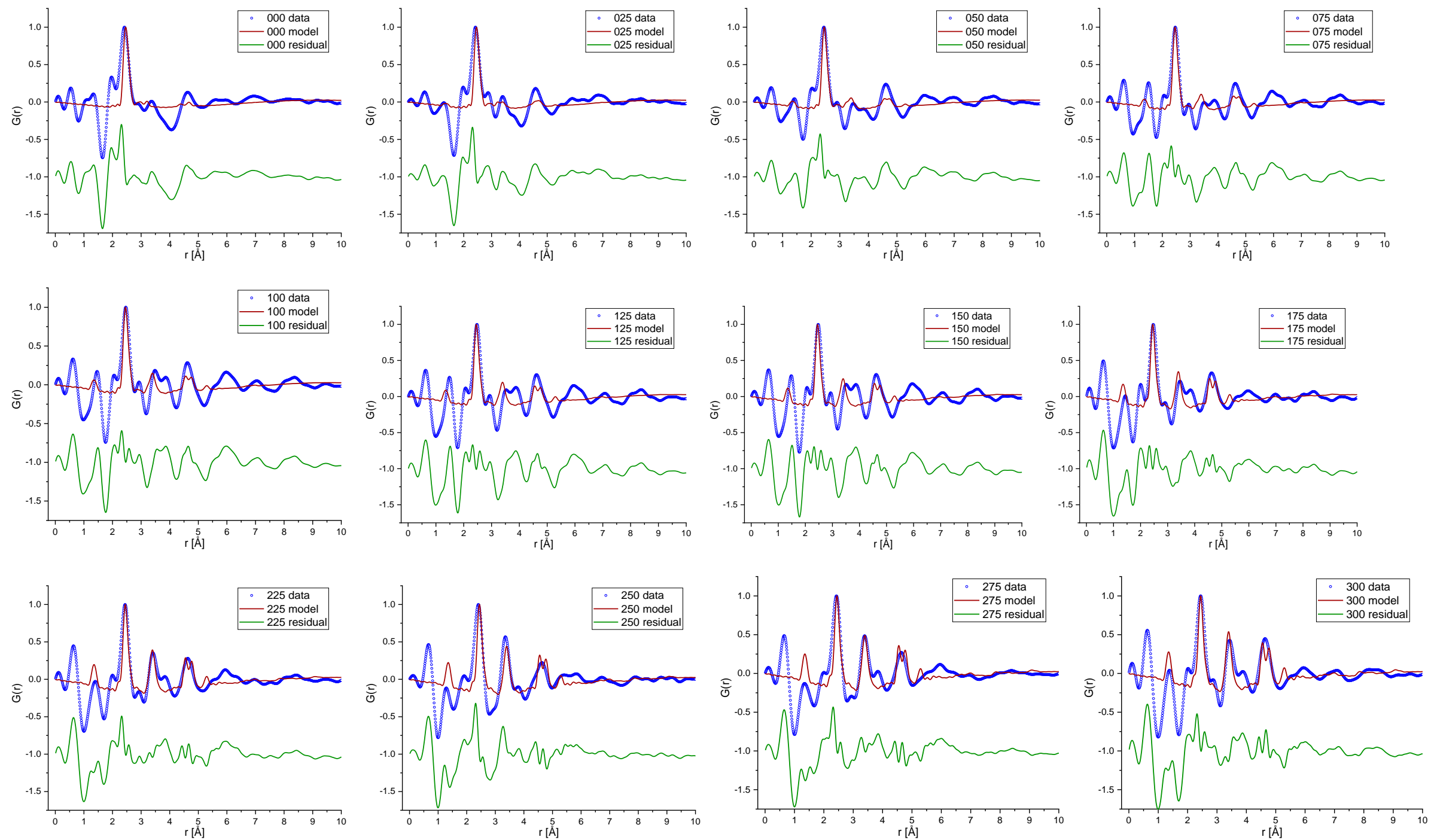


Figure S47 - Data, model and residuals of the europium(III) DPA titration series. Data is generated with $Q_{\max} = 13.5 \text{ \AA}^{-1}$ while the models are calculated with $Q_{\max} = 33.5 \text{ \AA}^{-1}$.

Transition energies

Table S3 - Transition energy offsets for observed absorption bands of $\text{Eu}(\text{DPA})_n^{3-2n}$

| $J \leftarrow J'$ | Line # | (0) | (1) | (2) | (3) |
|--|--------|---------|---------|---------|---------|
| ${}^5\text{H}_{4,6} \leftarrow {}^7\text{F}_0$ | 1 | 31385.6 | 31379.4 | 31404.9 | 31468.2 |
| | 2 | 31411 | 31383.4 | 31329.8 | 31357.5 |
| | 3 | 30936.9 | 31052.9 | 31120.4 | 31290.7 |
| | 4 | -- | -- | -- | 31091.1 |
| ${}^5\text{H}_3 \leftarrow {}^7\text{F}_0$ | 1 | 30500.8 | 30605.7 | 30436.1 | 30457.1 |
| ${}^5\text{D}_4 \leftarrow {}^7\text{F}_0$ | 1 | 27602.4 | 27593.7 | 27575.4 | 27582.3 |
| | 2 | -- | -- | -- | 27535.4 |
| ${}^5\text{L}_8 \leftarrow {}^7\text{F}_0$ | 1 | -- | 27249.8 | 27201 | 27228.1 |
| | 2 | -- | -- | -- | 27155.3 |
| ${}^5\text{G}_J, {}^5\text{L}_7 \leftarrow {}^7\text{F}_0$ | 1 | 26737.8 | 26540 | 26684.8 | 26609.4 |
| | 2 | 26580.7 | 26590.3 | 26551.9 | 26596 |
| | 3 | 26536.4 | 26536 | 26251.7 | 26509.9 |
| | 4 | 26434.6 | 26210.9 | 25945.6 | 26166.6 |
| | 5 | 26303.7 | 25915.5 | 25728.7 | 26063.3 |
| | 6 | 26146.5 | 25920.1 | 25662.6 | 25963.3 |
| | 7 | 26032.6 | 25764.6 | -- | 25879.5 |
| | 8 | 25829.8 | -- | -- | 25757.4 |
| | 9 | -- | -- | -- | 25546.3 |
| ${}^5\text{L}_6 \leftarrow {}^7\text{F}_{0,1}$ | 1 | 25338.3 | 25237.1 | 25230.1 | 25193.3 |
| | 2 | 25165.6 | 25169.4 | 25157.2 | 25037.6 |
| | 3 | 25042 | 25090.9 | 25031.5 | 24996.9 |
| | 4 | -- | -- | 14918.1 | 24929.2 |
| ${}^5\text{D}_2 \leftarrow {}^7\text{F}_0$ | 1 | 21494.8 | 21486.5 | 21475.9 | 21460.3 |
| ${}^5\text{D}_1 \leftarrow {}^7\text{F}_0$ | 1 | 19019.2 | 19031.5 | 18981.6 | 18984.8 |
| | 2 | -- | -- | -- | 18961.4 |
| ${}^5\text{D}_1 \leftarrow {}^7\text{F}_1$ | 1 | -- | 19003.4 | 18636.2 | 18643.7 |
| | 2 | -- | 18699 | 18603.7 | 18519.7 |
| ${}^5\text{D}_0 \leftarrow {}^7\text{F}_0$ | 1 | -- | 17272.4 | 17245.4 | -- |

Table S4 - Transition energy onset for observed emission bands of $\text{Eu}(\text{DPA})_n^{3-2n}$

| $J \rightarrow J'$ | Line # | [0] | [1] | [2] | [3] |
|---|--------|----------|---------|---------|---------|
| ${}^5\text{D}_0 \rightarrow {}^7\text{F}_0$ | 1 | - | 17220.8 | 17206.1 | 17201.1 |
| ${}^5\text{D}_0 \rightarrow {}^7\text{F}_1$ | 1 | 16987.84 | 16944 | 16949.7 | 16935.3 |
| | 2 | 16924.35 | 16877 | 16832 | 16820.9 |
| | 3 | - | - | 16848 | - |
| ${}^5\text{D}_0 \rightarrow {}^7\text{F}_2$ | 1 | 16355.3 | 16321.8 | 16306.7 | 16223 |
| | 2 | 16297.82 | 16253.4 | 16250.5 | - |
| | 3 | 16107.3 | - | - | - |
| ${}^5\text{D}_0 \rightarrow {}^7\text{F}_3$ | 1 | 15400.9 | 15371.4 | 15369.4 | 13571.5 |
| | 2 | - | - | 15354.6 | 15311 |
| | 3 | - | - | - | 15313.5 |
| ${}^5\text{D}_0 \rightarrow {}^7\text{F}_4$ | 1 | 14561.5 | 14546.5 | 14542.4 | 14537.5 |
| | 2 | 1445.38 | 14451.2 | 14443.9 | 14408.3 |
| | 3 | 14392 | 14408.6 | 14370.9 | 14350.3 |
| | 4 | 14371 | 14224.1 | 14235.9 | 14194.4 |

Emission probabilities ${}^5D_0 \rightarrow {}^7F_J, J = 0-6$

Table 5 – Average emission band probabilities of europium(III): Integrated area of the emission bands observed in the deconvoluted emission spectra.

| $J \rightarrow J'$ | Average emission band transition probabilities, $A_{rel} [s^{-1}]$ | | | |
|--------------------|--|-------|-------|-------|
| | [0] | [1] | [2] | [3] |
| $0 \rightarrow 0$ | -- | 0.71 | 0.40 | 0.02 |
| $0 \rightarrow 1$ | 3.74 | 6.45 | 8.11 | 6.30 |
| $0 \rightarrow 2$ | 1.26 | 11.59 | 22.13 | 22.58 |
| $0 \rightarrow 3$ | -- | 0.11 | 0.35 | 0.24 |
| $0 \rightarrow 4$ | 3.21 | 6.78 | 8.23 | 6.36 |
| $0 \rightarrow 5$ | -- | -- | -- | 0.09 |
| $0 \rightarrow 6$ | -- | 0.61 | 0.75 | 0.85 |

Table 6 – Average transition line probabilities of europium(III): Integrated area of the emission bands observed in the deconvoluted emission spectra, divided by the degeneracy of the emissive state.

| $J \rightarrow J'$ | Average spectral line transition probability, $A_{rel} [s^{-1}]$ | | | |
|--------------------|--|------|------|------|
| | [0] | [1] | [2] | [3] |
| $0 \rightarrow 0$ | -- | 0.71 | 0.40 | 0.02 |
| $0 \rightarrow 1$ | 1.25 | 2.15 | 2.70 | 2.10 |
| $0 \rightarrow 2$ | 0.25 | 2.32 | 4.43 | 4.52 |
| $0 \rightarrow 3$ | -- | 0.02 | 0.05 | 0.03 |
| $0 \rightarrow 4$ | 0.36 | 0.75 | 0.91 | 0.71 |
| $0 \rightarrow 5$ | -- | -- | -- | 0.01 |
| $0 \rightarrow 6$ | -- | 0.05 | 0.06 | 0.07 |